

1 The Role of direct Asphaltene Inhibitors on Asphaltene 2 Stabilization during Gas Injection

3 ¹Asgar Gandomkar*, ²Hamid Reza Nasriani

4 ¹ Department of Chemical and Petroleum Engineering, Faculty of Chemical and Material Engineering, Shiraz
5 Branch, Islamic Azad University, Shiraz, Iran
6

7 ²School of Engineering, Faculty of Science and Technology, University of Central Lancashire, Preston, PR1 2HE,
8 United Kingdom
9

10 **Abstract**

11 There are a large number of investigations, which evaluate the impact of the liquid-based
12 inhibitors on the asphaltene stabilization. In those studies, a specific volume of inhibitor was
13 added to the oil sample and the asphaltene precipitation is then studied. However, this method is
14 indirectly applicable to processes like gas injection. For that reason, in this work, the metal oxide
15 nanoparticles (GO, TiO₂, SiO₂, and MgO) have been considered in the liquid-free mode as direct
16 asphaltene inhibitors (DAIs) on asphaltene stabilization for the duration of miscible CO₂
17 injection. The dissolution of DAIs in CO₂ was investigated by measurement of cloud point
18 pressure to evaluate the pressure/temperature conditions, need for certifying that the CO₂/DAIs
19 mixtures have the single-phase condition. Afterwards, the impact of DAI was studied on
20 asphaltene precipitation and deposition by static and dynamic approaches. Results show that the
21 total size of asphaltene particles which precipitated during injection of miscible CO₂/DAIs
22 mixture is significantly lower than that for immiscible pure CO₂ injection. The amount of
23 asphaltene deposition significantly decreased during injection of miscible CO₂/DAIs mixtures
24 compared to immiscible pure CO₂ injection. Additionally, the metal oxide nanoparticles hinder

* **Corresponding Author**

Email Addresses: agandomkar@shirazu.ac.ir (Asgar Gandomkar)

1 the phase separation of asphaltenes kinetically and prevent growth. It is conducted by stabilizing
2 the colloidal suspension of the asphaltene particles, which are in sub-micrometre size to
3 significantly slow the asphaltene flocculation onset.

4 **Keywords:** CO₂ Injection, Asphaltene Stabilization, Direct Asphaltene Inhibitors, Cloud Point
5 Pressure, Metal Oxide Nanoparticles.

6 **1. Introduction**

7 The application of different substances, which efficiently stabilize or solubilize asphaltene in
8 crude oils, is both preventive and remedial measures, additionally; it saves costs and eases its
9 application during gas injection ([Joonaki et al., 2019](#); [Leonar et al., 2013](#); [Stephenson, 1990](#)).
10 Asphaltene precipitation/deposition is encountered during gas injection due to changes in reservoir
11 oil composition. The asphaltene deposition leads to reservoir wettability alteration, formation
12 damage, plugging of the wellbore and downhole facilities, consequently, it will harm the project
13 economics because of delays in production and expensive clean-up operations. The impact of
14 chemical inhibitors on the asphaltene stabilization during CO₂ flooding has been investigated
15 thoroughly. Several chemical products have been developed and investigated. The chemical
16 inhibitors are mainly selected based on their efficiency, availability, and environmental impacts.
17 The inhibitors are commonly categorized based on their molecular structures, chemical
18 characteristic, functional groups, alkyl tails, and aromaticity factor ([Yin et al., 2000](#)). There are
19 numerous studies in the literature which investigate the impact of liquid-based inhibitors on the
20 asphaltene stabilization in crude oil samples ([Hong et al., 2004](#); [Kazemzadeh et al., 2015](#); [Lu et](#)
21 [al., 2016](#); [Bae et al., 2016](#); [Shojaati et al., 2017](#); [Varamesh et at., 2019](#)). For example, Rocha et
22 al., ([2006](#)) studied a large number of asphaltene inhibitors, e.g. ethoxylated nonylphenols,
23 organic acids, dodecylbenzene sulfonic acid (DBSA), salicylic acid, and vegetable oils. They

1 reported a significant solubilization effect by DBSA. This finding highlighted the significant
2 impact of acid-base interactions. In addition, Hu et al., (2005) illustrated that nut oils have an
3 acceptable effectivity in the inhibition processes. Besides, Taher et al., (2002) considered
4 different chemicals as asphaltene inhibitors, i.e., DBSA, deasphalted crude oil (DO), resins (R),
5 toluene (T), the nonylphenol (NP) and dodecyl risol sinol (DR). Consequently, the capability of
6 the aforementioned chemicals on the inhibition of the asphaltene deposition was in this manner:
7 $DR > DBSA > NP > R > T > DO$. Moreover, the combination of DO and T at 60 weight percent
8 performed satisfactorily and the impact of NP and DBSA was analogous to DR. Joonaki et al.,
9 (2020) considered an asphaltenic oil mixed with a wax inhibitor-containing oil to investigate the
10 interaction of asphaltenes and waxes using the quartz crystal microbalance technique. They
11 showed that the different wax inhibitor chemistries illustrated different outcomes regarding the
12 asphaltene deposition tendency and lead to change the pour point and oil viscosity. Reubush
13 (1999) investigated some other chemicals as asphaltene inhibitors, the chemicals were as follow:
14 carboxylic and sulfonic acids, ethoxylated alcohols, phenols, and amines. They concluded that
15 ethoxylated alcohols and phenols are the best inhibitors. Hong et al., (2004) studied the impact of
16 two inhibitors: an anionic surfactant (sodium dodecyl sulfate) and a cationic surfactant
17 (cetylpyridinium chloride). It was evident that the combination of an alkane tail with acidic
18 functional group improved the asphaltene inhibition performance. Kelland (2009) reported that
19 nonylphenol (NP) has a decent inhibition capability on asphaltene aggregation; this is because
20 the OH functional group and alkane tail with 9 carbons are attached to the benzene ring. If
21 phenol and nonylphenol are compared, it highlights the effect of polar group and alkanes tail
22 length in the inhibitor. In the literature, the liquid-based chemicals were generally utilized and
23 were added to the crude oil or chemical solution that was injected into the reservoir. For

1 example, Ibrahim et al., (2004), Hassanpour et al., (2016 and 2018), and Varamesh et al., (2019)
2 were added the CO_3O_4 , toluene, TiO_2 , and $\text{NiO/Fe}_3\text{O}_4$ nanoparticles as inhibitors, respectively, to
3 the Saskatchewan and Asmari reservoir crude oils. Moreover, in the case of chemical solution
4 flooding into the reservoir cores, Lu et al., (2016) inspected the impact of Al_2O_3 nanoparticles on
5 the asphaltene deposition by conducting core flood experiments. The coreflooding results
6 indicated that the Al_2O_3 /nanofluid injection can hinder the asphaltene precipitation in porous
7 medium and consequently the reservoir permeability does not decrease. In addition, the
8 simultaneous injection of CO_2 and nano-fluid is more sufficient than the cyclic injection. Also,
9 Karambeygi et al., (2016) indicated that the salicylic acid can inhibit the asphaltene precipitation.
10 In addition, the high polar/aromatic inhibitors are similar to natural state of the resins which can
11 keep asphaltene particles in solution. Joonaki et al., (2017) investigated the asphaltene
12 precipitation using a quartz crystal microbalance technique to provide the most suitable scenario
13 for injection of commercial inhibitors/solvent at field conditions. Their results illustrated that the
14 reservoir conditions (pressure and temperature) and presence of gas might change the ranking of
15 commercial inhibitors for reducing the asphaltene precipitation. Consequently, the conventional
16 treatment of asphaltene precipitation/deposition is categorized into two methods during gas
17 injection: (a) the liquid-based chemical was added to the crude oil samples as asphaltene
18 inhibitors and (b) the gas alternating chemical solution (inhibitors) injection into the reservoir.
19 The first case is not applicable in the field scale and just illustrates the performance of the
20 inhibitor on asphaltene stabilization in crude oils. Also, the second scenario can be used in field-
21 scale, but it involves three-phase flow. Three-phase displacement (oil, gas, and chemical
22 solution) can be provided with some limitation during gas injection. The process is highly
23 affected by gravity at higher gas mobility and the gas/chemical solution gravity segregation can

1 play a negative role in this process. However, in our previous work ([Azizkhani and Gandomkar,](#)
2 [2020](#)), liquid-free chemicals have been used as direct asphaltene inhibitors through CO₂ injection
3 for the first time. This method involves two-phase flow displacement along with the inhibitor.
4 Based on our previous work, the metal oxide nanoparticles (Fe₃O₄ and Al₂O₃) were considered
5 as inhibitors while CO₂ injection. Subsequently, the asphaltene stabilization through
6 CO₂/nanoparticles injection was investigated using static precipitation tests for two different live
7 oil samples, i.e., volatile and intermediate live oil. Furthermore, it was noted that the amount of
8 asphaltene precipitation was mitigated when CO₂/nanoparticles was injected compared to the
9 case when pure CO₂ was injected. In addition, the mixtures that contain Fe₃O₄ could perform
10 better than Al₂O₃ solutions; therefore the impact of solubility is more dominant than the effect of
11 the aggregation during the injection of DAI. However, this study focused on asphaltene
12 deposition in carbonate reservoir cores by analyses of dynamic asphaltene tests. Four metal oxide
13 nanoparticles such as GO, TiO₂, SiO₂, and MgO were used as DAIs for asphaltene precipitation
14 to make the asphaltene more stable in the insitu oil sample during the injection of the carbon
15 dioxide. The cloud point pressure was monitored to ensure that the mixture of CO₂/nanoparticles
16 is single-phase. Once the impact of DAIs was studied on asphaltene deposition at the reservoir
17 conditions by static and dynamic asphaltene tests. This study considered a new approach for the
18 application of inhibitors in porous media during gas injection. This method can be performed for
19 other asphaltene inhibitors (alkaline and surfactant-based chemicals) as direct asphaltene
20 inhibitors.

21 **2. Materials and methods**

22 • **Direct asphaltene inhibitors (DAI)**

1 Four metal oxide nanoparticles such as the graphene oxide (GO, MW = 12.01 gr/mol), titanium
2 dioxide (TiO₂, MW = 79.87 gr/mol), silicon dioxide (SiO₂, MW = 60.08 gr/mol), and
3 magnesium oxide (MgO, MW = 40.3 gr/mol) were used as direct inhibitor agents to make the
4 asphaltene more stable in the reservoir live oil during the immiscible/miscible carbon dioxide
5 injection. The metal oxide nano-particles generally have acidic, basic or amphoteric chemical
6 characteristics, which causes polar interactions between asphaltenes molecules and nano-
7 particles. However, the chemical nature of metal oxide nanoparticles considered in this study is
8 acidic (SiO₂ and TiO₂) and basic (MgO and GO) (Nassar et al., 2011; Dai et al., 2014). All the
9 inhibitors are commercially available and were used in the experiment as they were received.
10 Different concentrations of nanoparticles were used in this study, i.e. 50, 100, 200, and 300 ppm
11 for GO and 500, 1000, 2000, and 3000 ppm for other DAIs. The SARA (Saturates, Aromatics,
12 Resins and Asphaltenes) analysis of reservoir crude oil with °API of 23.65 was reported in **Table**
13 **1**. The colloidal instability index (CII) was considered to investigate the instability of the crude
14 oil. It should be noted that the CII is an index which highlights the ratio of asphaltene and
15 saturate summation to the summation of resins and aromatics. If the CII value of a crude oil
16 sample is greater than 0.9, the crude oil is expressed as unstable (Ghloum et al., 2010 and 2019).
17 However, according to SARA data, the CII value for reservoir crude oils is 1.60, and it
18 demonstrates the asphaltene precipitation possibilities for these cases. However, in this work, the
19 recombined live oil was used in the experiments to study the asphaltene deposition at the
20 reservoir conditions. The results of a constant composition expansion (CCE) experiment were
21 used to guarantee that the recombined oil could represent the in-situ reservoir fluid with
22 acceptable accuracy. The CCE result illustrates that the measured bubble point pressure is

1 consistent with the real reservoir oil bubble point pressure ([Gandomkar et al., 2012](#)). The
2 reservoir pressure and temperature are 3150 psia and 60 °C, respectively.

3 **Table 1**

4

5 **• Cloud point pressure measurements**

6 The authors considered liquid-free additives as DAIs throughout CO₂ injection at the reservoir
7 conditions. The dissolution of DAIs (GO, TiO₂, SiO₂, and MgO) in CO₂ was investigated by
8 calculation of cloud point pressures. The cloud point appears the pressure at which cloudiness in the
9 solution is first observed as the pressure is lowered. It was measured by HPHT visual cell with
10 different concentrations based on our previous work ([Azizkhani and Gandomkar, 2020](#)). At first,
11 a determined amount of DAI is weighed out and insert into the window cell. After that, a
12 specified amount of CO₂ was added to the sample to provide the desired composition. The
13 mixture with constant total composition was pressurized and then used a magnetic stirrer to
14 create a rotating magnetic field (2000 rpm). It was continued to achieve single-phase solutions
15 from the window cell at favorable temperatures and pressures. Finally, the reduction in pressure
16 of all samples was considered at the intervals of 40 psi. The equilibrium condition took about
17 two hours to identify any visual changes. Also more time might be needed for the low solubility
18 materials. In general, the cloud point pressures of DAI/CO₂ were indicated in the fog form by
19 visual monitoring in the bulk sample ([Miller et al., 2009](#); [Lee et al., 2016](#)). The measurements
20 were repeated at least three times with reproducibility of ±5 psi. Subsequently, these mixtures
21 were considered in all experiments to certify that the single-phase solution has occurred.

22 **• Minimum miscibility pressure (MMP)**

1 The IFT measurements between the live oil and DAI/CO₂ were performed by the high-pressure
2 high-temperature IFT 700 apparatus. All the mixtures of hydrocarbon gas and DAIs were
3 provided and then used to measure the IFTs at reservoir conditions (i.e. 3150 psia and 60 °C). An
4 oil droplet is produced from the end of the capillary needle, which surrounded by pure CO₂ or
5 DAI/CO₂ at required conditions. However, the IFTs were measured using advanced drop shape
6 analysis software. In addition, the IFT error calculated via the standard deviation of 4 repeated
7 measurements of each mix, and it was about ± 0.1 . Also, the MMP measurement was conducted
8 using vanishing interfacial tension (VIT) procedure ([Azizkhani and Gandomkar, 2020](#); [Ghorbani
9 et al., 2014](#)).

10 • **Asphaltene precipitation, Static test**

11 To investigate the asphaltene precipitation throughout the injection of CO₂ and CO₂/DAI, the
12 PVT analysis was conducted. The PVT apparatus that was used in this study consisted the
13 followings: PVT cell, transfer container, back pressure regulation, air bath, HPLC pump,
14 sampling vessel, filter, recombination cell, and shaker. In the experiment, a certain volume of the
15 CO₂/DAI mixture was injected into the PVT cell that contained live oil at the reservoir
16 conditions. Next, the PVT cell was shaken for 24 hours at a chosen temperature and pressure.
17 Then, the mixture of the CO₂/DAI and live oil was then retained in a stationary position for
18 another day to ensure that the asphaltene precipitation was occurring. The crude oil sampling is
19 taken out for analysis of asphaltene precipitation during CO₂/DAI injection. High-pressure
20 filtration was used to separate the precipitated asphaltene from the oil at a constant pressure
21 during its displacement from the PVT cell into the sampling vessel. Subsequently, the IP 143
22 standard method was conducted to measure the amount of the asphaltene content of the sample
23 for all CO₂/DAI mixtures ([Azizkhani and Gandomkar, 2020](#); [Arciniegas et al., 2014](#)).

1 **3. Results and discussion**

2 The effect of GO, TiO₂, SiO₂, and MgO, as direct asphaltene inhibitors, on asphaltene
3 precipitation and deposition was studied during miscible CO₂ injection. The SARA analysis and
4 CII values were conducted to show the asphaltene precipitation possibilities for these cases.
5 Besides, the cloud point pressure of all the CO₂/nanoparticles mixtures was measured to ensure
6 that the single-phase conditions have occurred during asphaltene precipitation tests. Also, the
7 asphaltene precipitation and deposition investigated by static and dynamic tests, respectively at
8 reservoir conditions (i.e. 60 °C and 3150 psia).

9 • **Phase behavior of DAI/CO₂ by cloud point pressure measurements**

10 In **Table 3**, the cloud point pressures of CO₂ mixtures with GO, TiO₂, SiO₂, and MgO for
11 different temperatures of 25, 40, 60, and 80 °C is listed. It should be noted that, throughout cloud
12 point pressure measurements, the concentration of nano-particles were ranging from 50 to 300
13 ppm for GO and 500 to 3000 ppm for others. The cloud point pressures were ranging from 1400
14 to nearly 2500 psia. The cloud point pressure normally rises as the concentration of nano-
15 particles in the solution increases. Additionally, the cloud point pressures increase almost
16 linearly with increase in temperature. e.g., the cloud point pressures of GO illustrated that the
17 dissolution of direct asphaltene inhibitor in CO₂ has occurred at 1712, 1830, 1994, and 2159 psia
18 in different concentration; 50, 100, 200, and 300 ppm; respectively at reservoir temperature (i.e.
19 60 °C). According to these observations, all the cloud point pressures are lower than reservoir
20 pressure and consequently, the single-phase conditions occur during asphaltene
21 precipitation/deposition tests for all direct asphaltene inhibitors. The effect of temperature on the
22 cloud point pressure of CO₂/DAI is shown in **Figure 1** at different concentrations. Additionally,
23 the solubility of DAIs increase as the temperature decreases. This observation highlights that the

1 density is directly proportional to the solubility. It could be explained by the entropy of mixing
2 and its dependency to the temperature. The density of CO₂ reduces significantly at higher
3 temperatures, whereas the impact of temperature on the nanoparticles density is minimal. If the
4 density of CO₂ becomes significantly different from that of nanoparticles, the entropy of mixing
5 becomes negative and then the temperature has a converse impact on the system (Joung et al.,
6 2002). Based on these results, the cloud point pressures of GO are lower than other nanoparticles
7 considered in this study at the same temperature. The molecular weights of nanoparticles have an
8 impact on the solubility in CO₂, this is due to entropic impacts and coupled with the unwanted
9 enthalpy interactions related to the CO₂-phobic functionalities and CO₂ (Yu et al., 2014; Chu et
10 al., 2019). As it was observed, all the DAIs/CO₂ mixtures were single-phase at reservoir
11 conditions and then these solutions were used for all asphaltene precipitation experiments.

12 **Table 3**

13 **Figure 1**

14 **• MMP measurements**

15 The amount of asphaltene precipitation will be different during miscible and immiscible CO₂
16 injection. Cao et al., (2013) illustrated that the miscible CO₂ injection causes more asphaltene
17 precipitation compared to immiscible injection. However, in this study, vanishing interfacial
18 tension technique was used to investigate the effect of DAI on MMP. At first, at equilibrium
19 pressures ranging from 2500 to 3150 psia, the interfacial tension between live oil and pure/DAIs
20 CO₂ were assessed. It should be noted that all the IFT values were measured at the reservoir
21 temperature and pressures higher than the cloud point pressure to make sure that the mixtures of
22 the CO₂/Nanoparticles are single phase. In Table 4, the results of live oil-pure CO₂ and

1 DAI_s/CO₂ mixtures at T_{res}= 60 °C are listed. Considering the data of **Table 4**, the IFT for pure
2 CO₂, 200 ppm GO, 2000 ppm TiO₂, 2000 ppm SiO₂, and 2000 ppm MgO are 46, 13, 15, 14, and
3 15 dyne/cm, respectively at 2500 psia and 60 °C. The asphaltenes are known to be one of the
4 most surface-active compounds in crude oil and could be absorbed to the DAI_s surface and
5 reduce the IFTs. The metal oxide (DAI_s) surface will typically have high surface energy. It was
6 noted that GO could expressively decrease IFT compared to other DAI_s considered in this study.
7 It referred to the high specific surface area of GO compared to other DAI_s. In addition, an
8 increase in equilibrium pressure led to a significant reduction in IFT. It is well understood that as
9 the IFT between live oil and nanoparticles/carbon dioxide decreases it will increase the
10 miscibility and subsequently leads to a decrease in the residual oil saturation ([Ghorbani et al.,
11 2014](#)). As shown in [Figure 2](#), it is noted that MMP decreases as the concentration of the
12 nanoparticles increases. It is due to the fact that the density of the mixture of the nanoparticles
13 and CO₂ is slightly larger than the pure carbon-dioxide; this leads to a lower difference in density
14 with that of the live oil and therefore smaller IFT values than pure carbon-dioxide ([Chu et al.,
15 2019](#)). It is also shown that the MMP for GO/CO₂ is lower than that of the other mixtures. The
16 MMPs are 3370, 2941, 3006, 2938, and 3040 psia for pure CO₂, 200 ppm GO, 2000 ppm TiO₂,
17 2000 ppm SiO₂, and 2000 ppm MgO, respectively at reservoir temperature, 60 °C. Hence, the
18 MMP for pure CO₂ is above the P_{res}=3150 psi; and consequently, the immiscible conditions will
19 occur during pure CO₂ injection for asphaltene precipitation/deposition tests. Furthermore, the
20 MMPs for all CO₂/DAI_s are smaller than reservoir pressure, and as a result, miscible conditions
21 occur during static and dynamic asphaltene processes.

22 **Table 4**

23 **Figure 2**

1 • **PVT analysis of asphaltene precipitation through CO₂/DAI injection**

2 In this work, the team used nanoparticles as direct asphaltene inhibition agent to prevent the
3 asphaltene precipitation by static test during CO₂ injection. In all experiments, to guarantee that
4 all solutions are single-phase, the mixtures of CO₂/nanoparticles were injected at a pressure
5 higher than the cloud point pressure. The live oil has 6.4 weight percent initial asphaltene content
6 and from [Table 5](#), the amounts of 5.8 weight percent asphaltene precipitated during pure
7 immiscible injection of CO₂. It was expected that the amount of asphaltene precipitation
8 increases during miscible DAIs/CO₂ but it reduced using nanoparticles as direct asphaltene
9 inhibitors. The amount of asphaltene precipitation reduced from 5.8 to 3.1, 4.2, 4, and 3.8 weight
10 percent by using 100 ppm GO, 1000 ppm TiO₂, 1000 SiO₂, and 1000 ppm MgO mixtures,
11 respectively. Additionally, the CO₂/GO mixtures decreased the amounts of asphaltene
12 precipitation higher than other DAIs considered in this study. The specific surface area of the GO
13 (890 m²/g) is higher than that for TiO₂ (174.5 m²/g), SiO₂ (590 m²/g), and MgO (300 m²/g);
14 consequently, it led to more adsorption of asphaltene ([Yu et al., 2014](#); [Karambeygi et al., 2016](#);
15 [Chu et al., 2019](#)). The application of nanoparticles could enhance the solubility of asphaltene in
16 the live oil and consequently lead to a reduction in the precipitation of asphaltene. Likewise, it
17 increases the CO₂ solubility, dilutes the live oil, subsequently disperses the resin molecules, and
18 finally leads to asphaltene stabilization in oil. Also, the amounts of asphaltene precipitation
19 decreased by increasing DAI concentrations. The lone pair electrons, i.e., a pair of valence
20 electrons, of oxygen intensify the surface negative charge density of the metal oxide
21 nanoparticles, which enhances the adsorption of asphaltene fraction. It should be noted that there
22 is an insignificant reduction in asphaltene precipitation for the duration of a high concentration of
23 DAIs. For example, the amounts of asphaltene precipitation are 2.5 and 2.4 weight percent for

1 200 and 300 ppm GO, respectively. For that reason, the DAI concentration of 200 ppm can be
2 more efficient than other DAI concentrations through miscible CO₂/GO injection. It was
3 previously reported that the optimal concentration for Fe₃O₄ and TiO₂ nanoparticles in the
4 inhibitor is approximately one weight percent ([Hassanpour et al., 2018](#)). In addition, it will
5 decrease the asphaltene precipitation to seventeen and eighteen percent of initial content of
6 asphaltene using TiO₂ and Fe₃O₄ correspondingly. When a low concentration of inhibitor is
7 applied, active site on the structure of asphaltene could be occupied by free monomers and
8 consequently stabilizes the asphaltene particles within the solution ([Rocha et al., 2006](#)).
9 Additionally, the polar head group of the inhibitor has a dissimilar potential to attach to the
10 particles and makes the system of the inhibitor/asphaltene more stable. It should be highlighted
11 that these groups' polarity governs the strength of the bond. However, when a high concentration
12 of inhibitors is used, it will not lead to the desired result. As the inhibitors' concentration rises,
13 the likelihood of self-association under hydrogenous bonding increases accordingly. Conversely,
14 when a higher concentration of inhibitor is applied, the potential of self-association in inhibitor-
15 inhibitor is larger than the inhibitor/asphaltene's interaction. Consequently, the capability of
16 inhibitors on the stabilization of the asphaltenes decreases and it will cause the inhibitors to
17 underperform at higher concentrations ([Karambeygi, 2016](#); [Leon et al., 2001](#)). As a result, the
18 metal oxide nanoparticles have acidic/basic/amphoteric chemical characteristic, which causes
19 polar interactions between asphaltenes particles and nanoparticles. The bond formation between
20 nanoparticles (metal oxide) and asphaltene particles is a key factor that delays the beginning
21 point of separation of asphaltenes from oil, i.e., onset. The asphaltene particles could be
22 suspended in resins due to the formation bonding of metal-oxide nanoparticles and asphaltene
23 molecules and its bonding to the activated sites on the surface of the asphaltene particles ([Nassar](#)

1 et al., 2011). It should be noted there are two conflicting forces affecting the precipitation, i.e.,
2 aggregation effect and the solubility mechanism. The first force (aggregation effect) has a
3 tendency to lead to precipitation whilst the second (solubility mechanism) tends to retain the
4 asphaltene molecules in the solution. Furthermore, the results show that the impact of the
5 solubility mechanism is more dominant than that of the aggregation effect for the duration of the
6 injection of CO₂/nanoparticles (Gharbi et al., 2017; Rashid et al., 2019; Yen et al., 2001).

7 **Table 5**

8 • **The effect of DAI on asphaltene deposition**

9 The amount of asphaltene deposition into the carbonate cores was measured during coreflooding
10 tests for pure and CO₂/DAIs injection. Figure 3 shows the variation in the asphaltene content of
11 the produced oil with injected PV of pure and CO₂/DAIs injection during carbonate cores. The
12 asphaltene concentration in the oil was constant till CO₂ breakthrough which occurred at around
13 0.25 pore volumes (PV) and 0.35 PV for pure CO₂ and CO₂/DAIs mixtures, respectively.
14 Because the produced oil had not yet been in contact with the injected pure CO₂ and CO₂/DAIs,
15 the change in asphaltene content was insignificant. Inversely, the asphaltene content in the
16 produced oil after the CO₂ breakthrough reduced significantly. The drop in asphaltene content
17 highlights the fact that some further asphaltene precipitation/flocculation occurs in the carbonate
18 cores during pure and CO₂/DAIs injection. From Figure 3, the asphaltene content in produced oil
19 during injection of DAIs/CO₂ mixtures are higher than that for pure CO₂ injection. It shows that
20 the metal oxide nanoparticles can stabilize the asphaltene particles in reservoir oil. In addition,
21 the mixture of GO/CO₂ improved the asphaltene stabilization compared to other DAIs
22 considered in this study. From this result, the amount of asphaltene content in produced oil are
23 1.3, 5.4, 4.1, 3, and 5 weight percent after injection of 2 PV pure CO₂, 200 ppm GO, 2000 ppm

1 SiO₂, 2000 TiO₂, and 2000 ppm MgO mixtures, respectively. Also, [Figure 4](#) illustrates the
2 amount of asphaltene's deposition in the carbonate cores by the subtraction of the asphaltene
3 content in the produced oil from that of the initial crude oil during the dynamic tests. The amount
4 of asphaltene deposition significantly decreased during injection of CO₂/DAIs mixtures
5 compared to pure CO₂ injection. The metal oxide nanoparticles hinder the phase separation of
6 asphaltenes kinetically and prevent growth. It is conducted by stabilizing the colloidal
7 suspension of the asphaltene particles, which are in sub-micrometer size to significantly slow the
8 asphaltene flocculation onset. Consequently, the direct asphaltene inhibitors can prevent to
9 asphaltene deposition and act as asphaltene dispersants. The polyaromatic nuclei with aliphatic
10 side chains and rings of asphaltene connect and create micellar aggregates. This is well-
11 documented that in addition to aromatic compounds, asphaltenes consist of different acidic and
12 basic functional groups. The metal oxide nanoparticles that are adsorbed on the micelle core
13 make the asphaltene micelles more stable. The DAIs connects to the asphaltene particles using
14 their polar head and expands their aliphatic group outward. This creates a layer round
15 asphaltenes. On the condition that the asphaltene particles are stabilized in the micelles,
16 precipitation does not occur ([Setaro et al., 2019](#)).

17 **Figure 3**

18 **Figure 4**

19 Besides, using asphaltene particle size analysis approach, the team measured the mean size of the
20 asphaltene particles to study the impact of direct asphaltene inhibitors on asphaltene particle size
21 for the duration of pure CO₂ injection and 200 ppm GO/CO₂ mixture injection, [Figures 5](#) and [6](#).
22 Based on this result, the asphaltene particle size during pure CO₂ injection is higher than that for
23 GO/CO₂ mixture injection. It is clear that the GO/CO₂ mixtures can stabilize the asphaltene

1 particles in oil and significantly reduces the size of asphaltene particles simultaneously. The total
2 size of asphaltene particles which precipitated during the injection of pure CO₂ and 200 ppm
3 GO/CO₂ mixture are 2657808 and 756592 μm², respectively. The particles are created in two
4 different stages, i.e., phase separation stage and asphaltene particle growth stage. Phase
5 separation takes place when asphaltene particles in the oil precipitate and develop into large
6 aggregates. Additionally, the stability of asphaltene particles can be improved by the introduction
7 of compounds, which hold a polar head containing an acidic group, which can attach to the
8 micellar core. Dissimilar acidities are observed for amphiphiles with diverse head groups. The
9 inhibition capability of amphiphiles depends on the fact that how strong are their groups' acidity,
10 therefore the amphiphiles stabilize the asphaltene in the solution via the acid-base interaction.
11 The ability of amphiphiles' inhibition is related to the strength of these groups acidity and
12 illustrating that the asphaltene stabilization occurs through the acid-base interaction ([Zanganeh et](#)
13 [al., 2018](#)). However, direct asphaltene inhibitors can decrease the amount of asphaltene
14 precipitation and also prevents the aggregation of precipitated asphaltene particles. By the way,
15 the size of deposited asphaltene particles can affect the oil flow in porous media due to changing
16 the pressure drop. Based on the dynamic tests, the differential pressure during the pure CO₂
17 injection was higher than that for injection of CO₂/DAIs mixtures. It referred to asphaltene
18 precipitation, which increased formation damage during the pure CO₂ injection compared to
19 other cases. [Figure 7](#) shows the schematic of asphaltene deposition on the rock surface. The
20 asphaltenes may adsorb onto the rock surface and cause permeability blockage, wettability
21 alteration to oil-wet, reduces the oil effective permeability; and thereby decreases the oil
22 recovery ([Figure 7a](#)). However, the application of direct asphaltene inhibitors can stabilize the
23 asphaltene particles and also prevent to asphaltene deposition as a dispersant ([Figure 7b](#)).

1 Additionally, the presence of the metal oxide nanoparticles as direct asphaltene inhibitors can
2 enhance the oil recovery factor between 6 to 25 percent compared to pure CO₂ injection. The
3 adsorption performance of asphaltenes on the metal oxide nanoparticles is governed by two
4 properties, i.e., the surface energy and the structure of nanoparticles and the chemical and
5 physical characteristics of the asphaltene particles and polar, electrostatic, and van der Waals
6 interactions are the key factors which influence the asphaltene adsorption onto the solid surfaces.
7 Among these three factors, the acid–base (polar) and electrostatic interaction are the most
8 significant factors. It is well-documented that surface Gibbs energy reduced by the adsorption of
9 asphaltene particles on the nanoparticles. Consequently, the nanoparticles containing asphaltene
10 (which are adsorbed onto the surface of nanoparticles) have a weaker interaction compared to
11 those of the nanoparticles lacking asphaltene particles. Hence, the adsorbed asphaltene particles
12 onto the nanoparticles have higher stability in the reservoir rock ([Hosseinpour et al., 2013](#);
13 [Castro et al., 2009](#)). Throughout the CO₂/DAIs injection, the nanoparticles adsorb the
14 precipitated asphaltene particles and consequently alleviate the rate of the adsorption of
15 precipitated asphaltenes onto the rock surface and consequent deposition in the porous medium.
16 For that reason, the nanoparticles carrying asphaltenes could travel within the porous medium
17 and subsequently lead to inhibit the precipitation and as a result, prevents permeability reduction
18 due to asphaltene precipitation.

19 **Figure 5**

20 **Figure 6**

21 **Figure 7**

22

1 **4. Conclusions**

- 2 • Liquid-free inhibitors can be directly applicable for gas-based enhanced oil recovery in
3 field scale.
- 4 • The metal oxide nanoparticles could increase the stability of the colloidal asphaltenes and
5 consequently diminish the growing and the formation of flocculated asphaltene particles.
- 6 • The total size of asphaltene particles, which precipitated during injection CO₂/DAIs
7 mixture, is significantly lower than that for pure CO₂ injection.
- 8 • The effectiveness of the graphene oxide nanoparticle is much better than other DAIs in
9 retaining the asphaltene particles suspended and spread within the oil.
- 10 • The application of CO₂/GO mixtures could reduce the asphaltene aggregation/deposition
11 and improved the oil recovery factor between 6 to 25 percent compared to the case that
12 only CO₂ was injected.
- 13 • The cloud point pressure of CO₂/DAIs mixtures is under the reservoir pressure to certify
14 that the single-phase solution has occurred at reservoir conditions.
- 15 • The direct asphaltene inhibitors lead to a decrease in the IFT and provide the miscible
16 injection of gas at reservoir pressure and temperature.
- 17 • The metal oxide nanoparticles improved the solubility of the asphaltene particles and
18 consequently kept them in the solution.

19
20
21
22
23

- 1 **Nomenclature**
- 2 Colloidal Instability Index, CII
- 3 Constant Composition Expansion, CCE
- 4 Cubic Plus Association Equation of state, CPA
- 5 Deasphalted Crude Oil, DO
- 6 Direct Asphaltene Inhibitor, DAI
- 7 Dodecyl Benzene Sulfonic Acid, DDBSA
- 8 Dodecyl Risolsinol, DR
- 9 Graphene Oxide, GO
- 10 High-Pressure High-Temperature, HPHT
- 11 Liquefied Petroleum Gas, LPG
- 12 Magnesium Oxide, MgO
- 13 Minimum Miscibility Pressure, MMP
- 14 Nonyl Phenol, NP
- 15 Pressure, Volume, Temperature, PVT
- 16 Resins, R
- 17 Saturates, Aromatics, Resins, and Asphaltenes, SARA
- 18 Silicon Dioxide, SiO₂
- 19 Titanium Dioxide, TiO₂
- 20 Toluene, T
- 21 Vanishing Interfacial Tension, VIT
- 22 Weight percent, wt
- 23

1 **References**

2 Arciniegas, L.M., Babadagli, T., Asphaltene precipitation, flocculation and deposition
3 during solvent injection at elevated temperatures for heavy oil recovery, Fuel Journal, 124, 202-
4 211, 2014.

5 Azizkhani A., Gandomkar, A., A novel method for application of nanoparticles as direct
6 asphaltene inhibitors during miscible CO₂ injection, Journal of Petroleum Science and
7 Engineering, 185, 106661, 2020.

8 Bae, J., Fouchard, D., Garner, S., Macias, J., Advantages of Applying a Multifaceted
9 Approach to Asphaltene Inhibitor Selection, OTC 27171, 2016.

10 Cao, M., Gu, Y., Oil recovery mechanisms and asphaltene precipitation phenomenon in
11 immiscible and miscible CO₂ flooding processes, Fuel Journal, 109, 157-166, 2013.

12 Castro, M., Cruz, J.L., Ramirez, S., Villegas, A., Predicting adsorption isotherms of
13 asphaltenes in porous materials, Fluid Phase Equilibria, 286, 113-119, 2009.

14 Chu, T.M., Nguyen, N.T., Vu, T.L., Pham, T.D., Synthesis, Characterization, and
15 Modification of Alumina Nanoparticles for Cationic Dye Removal, Materials, 12, 450, 1-15,
16 2019.

17 Dai, J.F., Wang, G.J., Wu, Ch., Investigation of the Surface Properties of Graphene
18 Oxide and Graphene by Inverse Gas Chromatography, Chromatographia journal, 77, 299-307,
19 2014.

1 Gandomkar, A., Kharrat, R., Tertiary FAWAG Process on Gas and Water Invaded Zones,
2 an Experimental Study, Journal of Energy Sources, Part A: Recovery, Utilization, and
3 Environmental Effects, 34, 1913-1922, 2012.

4 Gandomkar, A., Rahimpour, M.R., Investigation of low salinity waterflooding in
5 secondary and tertiary enhanced oil recovery in limestone reservoirs, Energy & Fuels Journal,
6 29, 7781-7792, 2015.

7 Gharbi, Kh., Benyounes, Kh., Khodja, M., Removal and prevention of asphaltene
8 deposition during oil production: A literature review, Journal of Petroleum Science and
9 Engineering, 158, 351-360, 2017.

10 Ghloum, E.F., Qahtani, M.A., Rashid, A., Effect of inhibitors on asphaltene precipitation
11 for Marrat Kuwaiti reservoirs, Journal of Petroleum Science and Engineering, 70, 99-106, 2010.

12 Ghloum, E.F., Rashed, A.M., Safa, M.A., Mitigation of asphaltene precipitation
13 phenomenon via chemical inhibitors, Journal of Petroleum Science and Engineering, 175, 495-
14 507, 2019.

15 Ghorbani, M., Momeni, ., Safavi, S., Gandomkar, A., Modified Vanishing Interfacial
16 Tension (VIT) Test for CO₂-Oil Minimum Miscibility Pressure (MMP) Measurement, Journal of
17 Natural Gas Science and Engineering, 20, 92-98, 2014.

18 Hassanpour, S., Malayeri, M.R., Riazi, M., Utilization of CO₃O₄ nanoparticles for
19 reducing precipitation of asphaltene during CO₂ injection, Journal of Natural Gas Science and
20 Engineering, 31, 39-47, 2016.

1 Hassanpour, S., Malayeri, M.R., Riazi, M., Asphaltene Precipitation during Injection of
2 CO₂ Gas into a Synthetic Oil in the Presence of Fe₃O₄ and TiO₂ Nanoparticles, Journal of
3 chemical engineering data, 63 (5), 1266-1274, 2018.

4 Hong, E., Watkinson, P., A study of asphaltene solubility and precipitation. Fuel journal,
5 83, 1881-1887, 2004.

6 Hosseinpour, N., Khodadadi, A.A., Bahramian, A., Mortazavi, Y., Asphaltene adsorption
7 onto acidic/basic metal oxide nanoparticles toward in situ upgrading of reservoir oils by
8 nanotechnology, Langmuir, 29, 14135-14146, 2013.

9 Hu, Y.F., Guo, T.M., Effect of the structures of ionic liquids and alkylbenzenederived
10 amphiphiles on the inhibition of asphaltene precipitation from CO₂-injected reservoir oils,
11 Langmuir, 21, 8168-8174, 2005.

12 Ibrahim, H.H., Idem, R.O., Inter relationships between Asphaltene Precipitation Inhibitor
13 Effectiveness, Asphaltenes Characteristics, and Precipitation Behavior during n-Heptane (Light
14 Paraffin Hydrocarbon) -Induced Asphaltene Precipitation, Energy & Fuels, 18, 1038-1048, 2004.

15 Joonaki, E., Burgass, R., Hassanpouryouzband, A., Tohidi, B., Comparison of
16 experimental techniques for evaluation of chemistries against asphaltene aggregation and
17 deposition: new application of high-pressure and high-temperature quartz, Energy & Fuels, 32, 3,
18 2712-2721, 2017.

19 Joonaki, E., Buckman, J., Burgass, R., Tohidi, B., Water versus Asphaltenes; Liquid–
20 Liquid and Solid–Liquid Molecular Interactions Unravel the Mechanisms behind an Improved
21 Oil Recovery Methodology, Scientific Reports, 9, 1, 11369, 2019.

1 Joonaki, E., Hassanpouryouzband, A., Burgass, R., Hase, A., Tohidi, B., Effects of
2 Waxes and the Related Chemicals on Asphaltene Aggregation and Deposition Phenomena:
3 Experimental and Modeling Studies, ACS omega 5, 13, 7124-7134, 2020.

4 Joung, S.N., Park, J.U., Kim, S.Y., High-pressure phase behavior of polymersolvent
5 systems with addition of supercritical CO₂ at temperatures from 323.15 K to 503.15 K,
6 Journal of Chemical & Engineering Data, 47, 2, 270-273, 2002.

7 Karambeygi, M.A., Nikazar, M., Kharrat, R., Experimental evaluation of asphaltene
8 inhibitors selection for standard and reservoir conditions, Journal of Petroleum Science and
9 Engineering, 13, 74-86, 2016.

10 Kazemzadeh, Y., Malayeri, M.R., Riazi, M., Parsaei, R., Impact of Fe₃O₄ nanoparticles
11 on asphaltene precipitation during CO₂ injection, Journal of Natural Gas Science and
12 Engineering, 22, 227-234, 2015.

13 Kelland, M.A., Asphaltene control. Production Chemicals for the Oil and Gas Industry.
14 Stavanger, Norway: University of Stavanger, Chapter 4, 2009.

15 Leonard, G.Ch., Ponnepati, R., Rivers, G., Novel Asphaltene Inhibitor for Direct
16 Application to Reservoir, SPE 167294, 2013.

17 Leon, O., Contreras, E., Rogel, E., Dambakli, G., Espidel, J., Avedo, S., The influence
18 of the adsorption of amphiphiles and resins in controlling asphaltene flocculation, Energy and
19 Fuels, 15, 102-1032, 2001.

20 Lee, J.J., Dhuwe, A., Stephen, D., Eric, J., Enick, R.M., Polymeric and Small Molecule
21 Thickeners for CO₂, Ethane, Propane and Butane for Improved Mobility Control, SPE Improved
22 Oil Recovery Conference, Tulsa, SPE 179587, 2016.

1 Li, X., Guo, Y., Sun, Q., Lan, W., Guo, X., Experimental study for the impacts of flow
2 rate and concentration of asphaltene precipitant on dynamic asphaltene deposition in
3 microcapillary medium, *Journal of Petroleum Science and Engineering*, 162, 333-340, 2018.

4 Lu, T., Li, Zh., Fan, W., Zhang, X., Nanoparticles for Inhibition of Asphaltenes
5 Deposition during CO₂ Flooding, *Industrial & Engineering Chemistry Research*, 55 (23), 6723-
6 6733, 2016.

7 Miller, M.B., Chen, D.L., Xie, H.B., Luebke, D.R., Enick, R.M., Solubility of CO₂ in
8 CO₂-philic oligomers; cosmothem predictions and experimental results, fluid phase equilibria,
9 287, 26-32, 2009.

10 Nassar, N.N., Hassan, A., Pereira, A.P., Metal oxide nanoparticles for asphaltene
11 adsorption and oxidation, *Energy & Fuels*, 25, 3, 1017-1023, 2011.

12 Nguele, R., Ghulami, M.R., Sasaki, K., Asphaltene Aggregation in Crude Oils during
13 Supercritical Gas Injection, *Energy and Fuels*, 30, 2, 1266-1278, 2016.

14 Rappaport, L.A., Leas, W.J. 1953," Properties of Linear Waterfloods, presented at the Fall Meeting of the
15 Petroleum Branch in Houston, Texas, SPE 213-G.

16 Rashid, Z., Wilfred, C.D., Murugesan, Th., A comprehensive review on the recent advances on
17 the petroleum asphaltene aggregation, *Journal of Petroleum Science and Engineering*, 176, 249-
18 268, 2019.

19 Reubush, S. D., Effects of storage on the linear viscoelastic response of polymer-
20 modified asphalt at intermediate to high temperatures, MS Thesis, Virginia Polytechnic Institute
21 and State University, Blacksburg, VA, 1999.

1 Rocha, L.C., Ferreira, M.S., Ramos, A.C., Inhibition of asphaltene precipitation in
2 Brazilian crude oils using new oil soluble amphiphiles, *Journal of Petroleum Science and*
3 *Engineering*, 51, 26-36, 2006.

4 Setaro, L.O., Pereira, V.J., Costa, G.M., Melo, S., A novel method to predict the risk of
5 asphaltene precipitation due to CO₂ displacement in oil reservoirs, *Journal of Petroleum Science*
6 *and Engineering*, 176, 1008-1017, 2019.

7 Shojaati, F., Riazi, M., Mousavi, S.H., Experimental investigation of the inhibitory
8 behavior of metal oxides nanoparticles on asphaltene precipitation, *Colloids and Surfaces A:*
9 *Physicochemical and Engineering Aspects*, 531, 99-110, 2017.

10 Srivastava, R.K., Huang, S.S., Dong, M., Asphaltene Deposition During CO₂ Flooding,
11 *SPE Production & Facilities*, SPE 59092, 14, 4, 1999.

12 Stephenson, W.K., *Producing Asphaltene Crude Oils: Problems and Solutions*, *Petroleum*
13 *Engineer*, 24, 1990.

14 Taher, A.S., Mohammed, A.F., Amal, S.E., Retardation of asphaltene precipitation by
15 addition of toluene, resins, deasphalted oil and surfactants, *Fluid Phase Equilibria* 194-197,
16 1045-1057, 2002.

17 Varamesh, A., Hosseinpour, N., Prediction of Asphaltene Precipitation in Reservoir
18 Model Oils in the Presence of Fe₃O₄ and NiO Nanoparticles by Cubic Plus Association
19 Equation of State, *Industrial & Engineering Chemistry Research*, 58 (10), 4293-4302, 2019.

20 Yen, A., Yin, Y.R., Asomaning, S., Evaluating Asphaltene Inhibitors: Laboratory Tests
21 and Field Studies, SPE 65376, 2001.

1 Yin, Y.R., Yen, A.T., Asphaltene Deposition and Chemical Control in CO₂ Floods, SPE-
2 59293, 2000.

3 Yu, H., Li, Y., Fan, L., Yang, Sh., Highly dispersible and charge-tunable magnetic
4 Fe₃O₄ nanoparticles: facile fabrication and reversible binding to GO for efficient removal of dye
5 pollutants, Journal of Materials Chemistry A, 38, 2, 15763-15767, 2014.

6 Zanganeh, P., Dashti, .H, Ayatollahi, Sh., Comparing the effects of CH₄, CO₂, and N₂
7 injection on asphaltene precipitation and deposition at reservoir condition: A visual and
8 modeling study, Fuel, 217, 633-641, 2018.

9
10
11
12
13
14
15
16
17
18
19
20
21
22
23

1 **List of Tables**

2 **Table 1:** Reservoir oil properties

3 **Table 2:** Carbonate rock properties

4 **Table 3:** Cloud point pressure (psia) of CO₂ and GO, TiO₂, SiO₂, and MgO nanoparticles
5 mixtures at different nanoparticle concentrations at 25, 40, 60, and 80 °C

6 **Table 4:** IFT measurements of pure CO₂ and CO₂/nanoparticles with reservoir oil, at different
7 DAI concentrations at reservoir temperature ($T_{res}= 60$ °C), and MMP of these mixtures which
8 measured by VIT technique

9 **Table 5:** The effect of GO, TiO₂, SiO₂, and MgO nanoparticles on asphaltene precipitation as
10 direct asphaltene inhibitors during static test at reservoir conditions, 60 °C and 3150 psia

11

12

13

14

15

16

17

18

19

20

21

22

23

24

1
2
3
4
5
6
7
8
9
10
11
12
13
14
15
16
17

Table 1

Reservoir oil properties	Values
Saturates	55.10 wt
Aromatics	22.90 wt
Resins	15.60 wt
Asphaltenes	6.40 wt
CII	1.60
API	23.65
Molecular weight, g/mol, IP-86	164.80
S.G (60°F), ASTM-D40452	0.91
Acid Number, mg/g (KOH)	1.45
T _{res} (°C)	60
P _{res} (psia)	3150

1
2
3
4
5
6
7
8
9
10
11
12
13
14
15
16
17
18
19
20

Table 2

Limestone Cores No.	Length (cm)	Diameter (in)	PV (cc)	Helium Porosity (Percent)	Permeability (mD)	Connate Water (Percent)
C1	7.5	1.5	11.9	13.91	7.5	27.9
C2	7.4	1.5	12.5	14.81	8.2	29.5
C3	7.7	1.5	13.3	15.15	8.6	28.4
C4	7.8	1.5	13.0	14.61	7.8	29.1
C5	7.7	1.5	13.1	14.92	8.3	28.5

1
2
3
4
5

6
7
8
9
10
11
12
13
14
15

Table 3

DAI	Concentration (ppm)	Cloud point pressure (psia)			
		25 °C	40 °C	60 °C	80 °C
GO	50	1419	1538	1712	1935
	100	1527	1659	1830	2061
	200	1670	1812	1994	2215
	300	1746	1971	2159	2406
TiO ₂	500	1631	1724	1921	2126
	1000	1731	1862	2026	2243
	2000	1865	2028	2183	2388
	3000	1953	2159	2340	2589
SiO ₂	500	1574	1663	1859	2080
	1000	1653	1725	1938	2180
	2000	1785	1947	2105	2300
	3000	1883	2082	2265	2497
MgO	500	1469	1575	1755	1971
	1000	1579	1690	1884	2118
	2000	1720	1882	2058	2263
	3000	1792	2046	2217	2483

1
2
3
4
5
6
7
8
9
10
11
12

Table 4

DAI	Concentration (ppm)	IFT (dyn/cm) Live oil/CO ₂ -DAI, T _{res} = 60 °C				
		P=2500 psia	P=2800 psia	P=3000 psia	P _{res} =3150 psia	MMP (psia)
GO	Pure CO ₂	46	31	20	12	3370
	50	28	16	7	0	3100
	100	18	9	1	0	3049
	200	13	4	0	0	2941
	300	6	0	0	0	2740
TiO ₂	500	34	19	8	0	3140
	1000	22	11	3	0	3115
	2000	15	6	1	0	3006
	3000	9	1	0	0	2811
SiO ₂	500	31	16	5	0	3115
	1000	20	10	1	0	3027
	2000	14	4	0	0	2938
	3000	7	0	0	0	2761
MgO	500	30	19	8	0	3110
	1000	19	11	2	0	3100
	2000	15	7	0	0	3040
	3000	8	1	0	0	2814

1
2
3
4
5

6
7
8
9
10
11
12
13
14

Table 5

DAI	Concentration (ppm)	Asphaltene Precipitation, Static Test (wt%)
	Pure CO ₂	5.8
GO	50	4.0
	100	3.1
	200	2.5
	300	2.4
TiO ₂	500	5.0
	1000	4.2
	2000	3.8
	3000	3.7
SiO ₂	500	4.8
	1000	4.0
	2000	3.5
	3000	3.4
MgO	500	4.5
	1000	3.8
	2000	3.5
	3000	3.5

1 **List of Figures**

2 **Figure 1:** The impact of temperatures (25, 40, 60, and 80 °C) on cloud point pressures of DAI
3 (GO, TiO₂, SiO₂, MgO) and CO₂

4 **Figure 2:** The effect of DAI on Minimum miscibility pressure measured by the VIT technique at
5 reservoir temperature, T_{res}= 60 °C

6 **Figure 3:** The impact of direct asphaltene inhibitors (GO, TiO₂, SiO₂, MgO) on asphaltene
7 content of the produced oil during dynamic tests at reservoir conditions, 60 °C and 3150 psia

8 **Figure 4:** The impact of direct asphaltene inhibitors (GO, TiO₂, SiO₂, MgO) on asphaltene
9 deposition during dynamic tests at reservoir conditions, 60 °C and 3150 psia

10 **Figure 5:** Asphaltene particle size, which are precipitated during pure CO₂ injection at reservoir
11 conditions

12 **Figure 6:** Asphaltene particle size, which are precipitated during DAI/CO₂ injection at reservoir
13 conditions

14 **Figure 7:** The effect of DAI on asphaltene Deposition and decreasing the formation damage: a)
15 pure CO₂ injection and b) CO₂/DAIs injection

16

17

18

19

20

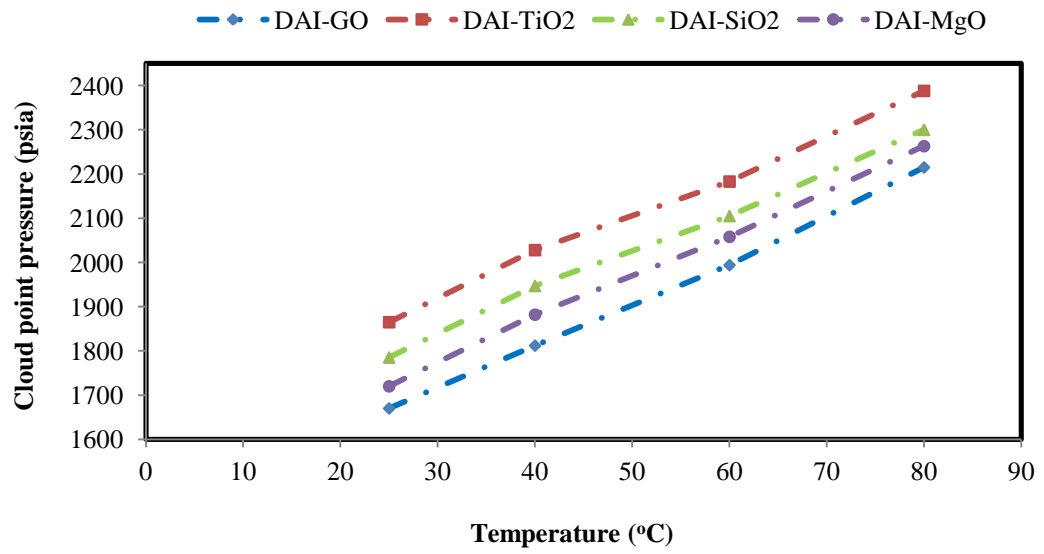
21

22

23

24

1
2
3
4



5
6
7
8
9
10
11
12
13
14
15
16
17

Figure 1

1
2
3
4

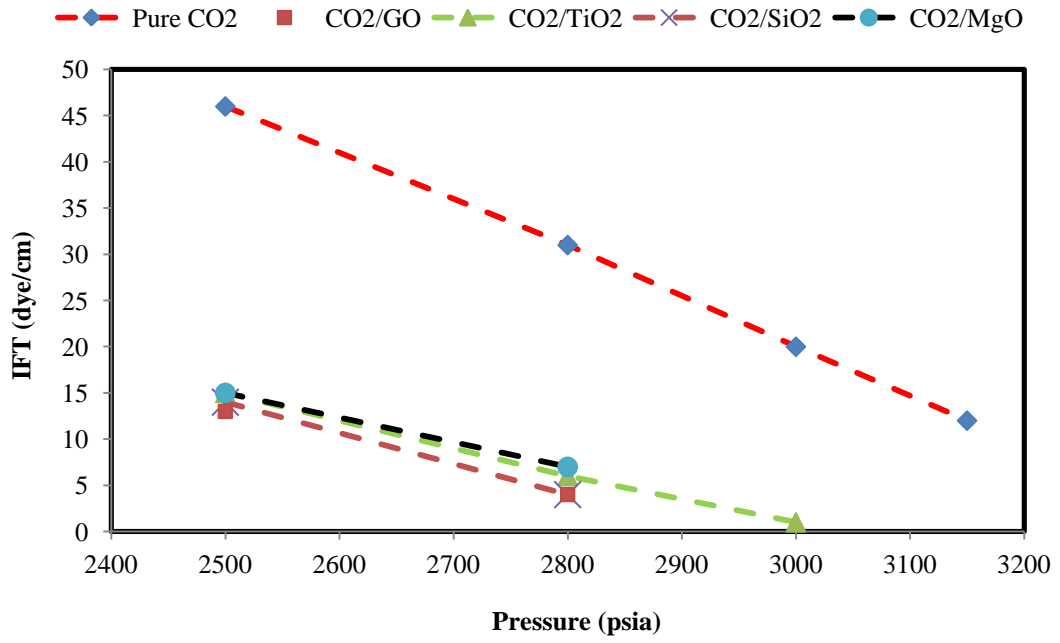


Figure 2

5
6
7
8
9
10
11
12
13
14
15
16

1
2
3
4

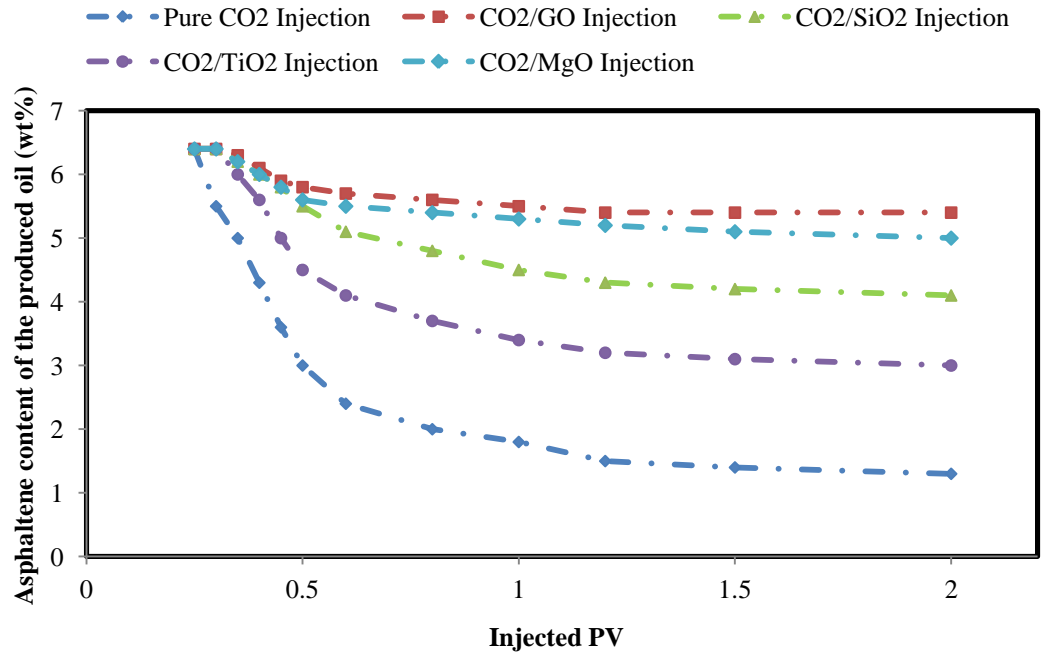
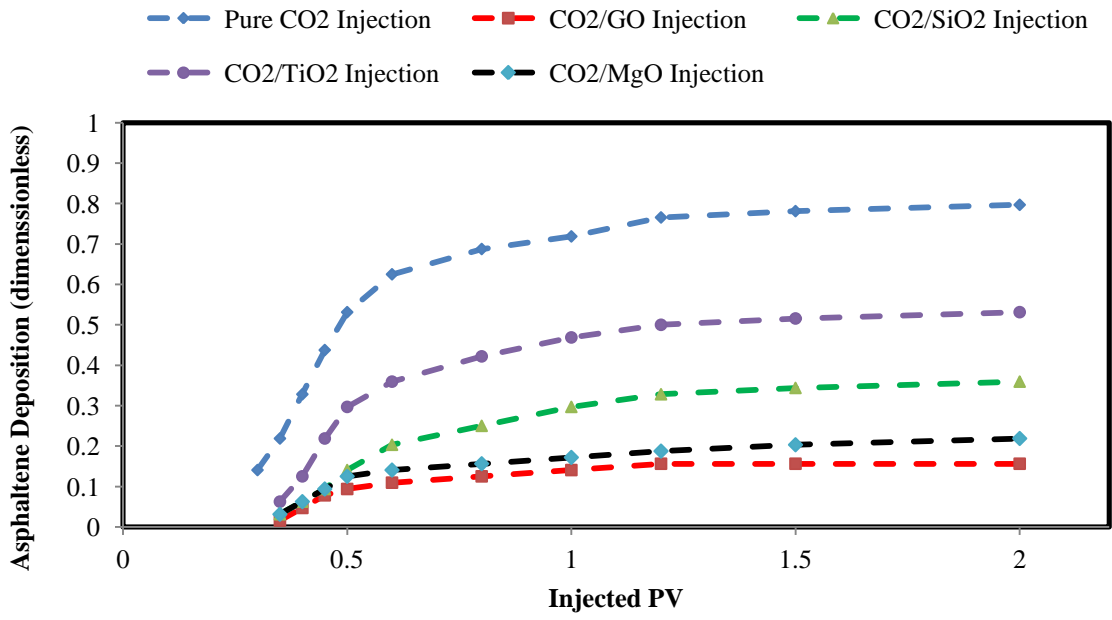


Figure 3

5
6
7
8
9
10
11
12
13
14
15

1
2
3
4
5



6
7
8
9
10
11
12
13
14

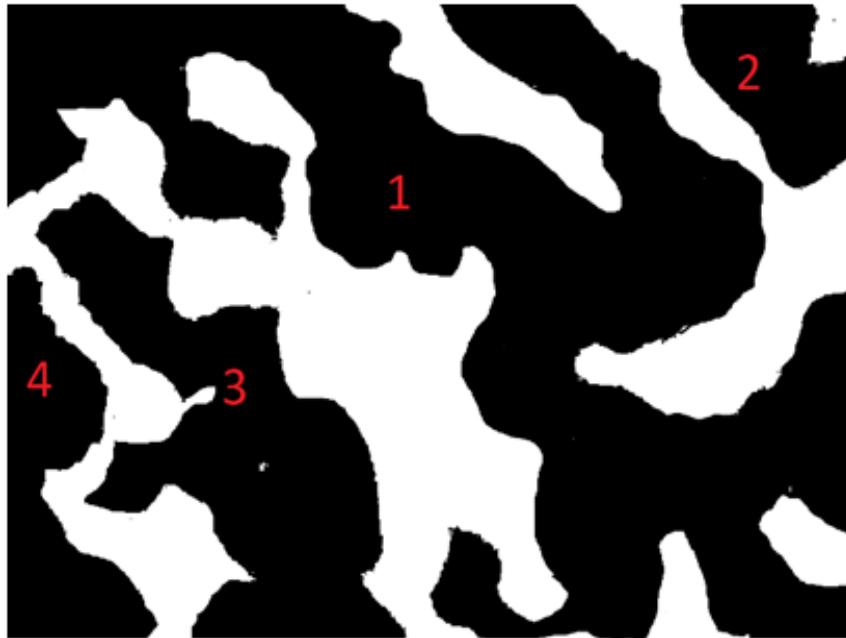
Figure 4

1

2

3

4



Particle number	1	2	3	4
Area (μm^2)	1741670	157860	534393	223885
Total area (μm^2)	2657808			

5

6

7

8

9

10

11

Figure 5

1
2
3
4
5
6

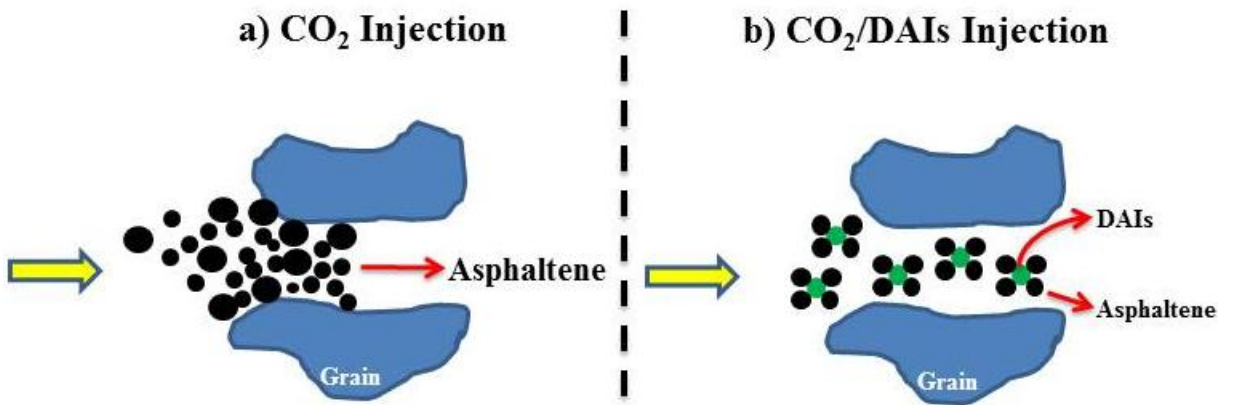


Particle number	1	2	3	4	5	6	7	8	9	10
Area (μm^2)	29798	74005	53573	73264	68014	102846	104938	75591	125733	48830
Total area (μm^2)	756592									

7
8
9
10
11
12
13
14
15
16
17

Figure 6

1
2
3
4
5
6



7
8
9
10
11
12

Figure 7

1 The Role of direct Asphaltene Inhibitors on Asphaltene 2 Stabilization during Gas Injection

3 ¹Asgar Gandomkar*, ²Hamid Reza Nasriani

4 ¹ Department of Chemical and Petroleum Engineering, Faculty of Chemical and Material Engineering, Shiraz
5 Branch, Islamic Azad University, Shiraz, Iran
6

7 ²School of Engineering, Faculty of Science and Technology, University of Central Lancashire, Preston, PR1 2HE,
8 United Kingdom
9

10 **Abstract**

11 There are a large number of investigations, which evaluate the impact of the liquid-based
12 inhibitors on the asphaltene stabilization. In those studies, a specific volume of inhibitor was
13 added to the oil sample and the asphaltene precipitation is then studied. However, this method is
14 indirectly applicable to processes like gas injection. For that reason, in this work, the metal oxide
15 nanoparticles (GO, TiO₂, SiO₂, and MgO) have been considered in the liquid-free mode as direct
16 asphaltene inhibitors (DAIs) on asphaltene stabilization for the duration of miscible CO₂
17 injection. The dissolution of DAIs in CO₂ was investigated by measurement of cloud point
18 pressure to evaluate the pressure/temperature conditions, need for certifying that the CO₂/DAIs
19 mixtures have the single-phase condition. Afterwards, the impact of DAI was studied on
20 asphaltene precipitation and deposition by static and dynamic approaches. Results show that the
21 total size of asphaltene particles which precipitated during injection of miscible CO₂/DAIs
22 mixture is significantly lower than that for immiscible pure CO₂ injection. The amount of
23 asphaltene deposition significantly decreased during injection of miscible CO₂/DAIs mixtures
24 compared to immiscible pure CO₂ injection. Additionally, the metal oxide nanoparticles hinder

* **Corresponding Author**

Email Addresses: agandomkar@shirazu.ac.ir (Asgar Gandomkar)

1 the phase separation of asphaltenes kinetically and prevent growth. It is conducted by stabilizing
2 the colloidal suspension of the asphaltene particles, which are in sub-micrometre size to
3 significantly slow the asphaltene flocculation onset.

4 **Keywords:** CO₂ Injection, Asphaltene Stabilization, Direct Asphaltene Inhibitors, Cloud Point
5 Pressure, Metal Oxide Nanoparticles.

6 **1. Introduction**

7 The application of different substances, which efficiently stabilize or solubilize asphaltene in
8 crude oils, is both preventive and remedial measures, additionally; it saves costs and eases its
9 application during gas injection ([Joonaki et al., 2019](#); [Leonar et al., 2013](#); [Stephenson, 1990](#)).
10 [Asphaltene precipitation/deposition](#) is encountered during gas injection due to changes in reservoir
11 oil composition. The asphaltene deposition leads to reservoir wettability alteration, formation
12 damage, plugging of the wellbore and downhole facilities, consequently, it will harm the project
13 economics because of delays in production and expensive clean-up operations. The impact of
14 chemical inhibitors on the asphaltene stabilization during CO₂ flooding has been investigated
15 thoroughly. Several chemical products have been developed and investigated. The chemical
16 inhibitors are mainly selected based on their efficiency, availability, and environmental impacts.
17 The inhibitors are commonly categorized based on their molecular structures, chemical
18 characteristic, functional groups, alkyl tails, and aromaticity factor ([Yin et al., 2000](#)). There are
19 numerous studies in the literature which investigate the impact of liquid-based inhibitors on the
20 asphaltene stabilization in crude oil samples ([Hong et al., 2004](#); [Kazemzadeh et al., 2015](#); [Lu et](#)
21 [al., 2016](#); [Bae et al., 2016](#); [Shojaati et al., 2017](#); [Varamesh et at., 2019](#)). For example, Rocha et
22 al., ([2006](#)) studied a large number of asphaltene inhibitors, e.g. ethoxylated nonylphenols,
23 organic acids, dodecylbenzene sulfonic acid (DBSA), salicylic acid, and vegetable oils. They

1 reported a significant solubilization effect by DBSA. This finding highlighted the significant
2 impact of acid-base interactions. In addition, Hu et al., (2005) illustrated that nut oils have an
3 acceptable effectivity in the inhibition processes. Besides, Taher et al., (2002) considered
4 different chemicals as asphaltene inhibitors, i.e., DBSA, deasphalted crude oil (DO), resins (R),
5 toluene (T), the nonylphenol (NP) and dodecyl risol sinol (DR). Consequently, the capability of
6 the aforementioned chemicals on the inhibition of the asphaltene deposition was in this manner:
7 $DR > DBSA > NP > R > T > DO$. Moreover, the combination of DO and T at 60 weight percent
8 performed satisfactorily and the impact of NP and DBSA was analogous to DR. Joonaki et al.,
9 (2020) considered an asphaltenic oil mixed with a wax inhibitor-containing oil to investigate the
10 interaction of asphaltenes and waxes using the quartz crystal microbalance technique. They
11 showed that the different wax inhibitor chemistries illustrated different outcomes regarding the
12 asphaltene deposition tendency and lead to change the pour point and oil viscosity. Reubush
13 (1999) investigated some other chemicals as asphaltene inhibitors, the chemicals were as follow:
14 carboxylic and sulfonic acids, ethoxylated alcohols, phenols, and amines. They concluded that
15 ethoxylated alcohols and phenols are the best inhibitors. Hong et al., (2004) studied the impact of
16 two inhibitors: an anionic surfactant (sodium dodecyl sulfate) and a cationic surfactant
17 (cetylpyridinium chloride). It was evident that the combination of an alkane tail with acidic
18 functional group improved the asphaltene inhibition performance. Kelland (2009) reported that
19 nonylphenol (NP) has a decent inhibition capability on asphaltene aggregation; this is because
20 the OH functional group and alkane tail with 9 carbons are attached to the benzene ring. If
21 phenol and nonylphenol are compared, it highlights the effect of polar group and alkanes tail
22 length in the inhibitor. In the literature, the liquid-based chemicals were generally utilized and
23 were added to the crude oil or chemical solution that was injected into the reservoir. For

1 example, Ibrahim et al., (2004), Hassanpour et al., (2016 and 2018), and Varamesh et al., (2019)
2 were added the CO_3O_4 , toluene, TiO_2 , and $\text{NiO/Fe}_3\text{O}_4$ nanoparticles as inhibitors, respectively, to
3 the Saskatchewan and Asmari reservoir crude oils. Moreover, in the case of chemical solution
4 flooding into the reservoir cores, Lu et al., (2016) inspected the impact of Al_2O_3 nanoparticles on
5 the asphaltene deposition by conducting core flood experiments. The **coreflooding** results
6 indicated that the Al_2O_3 /nanofluid injection can hinder the asphaltene precipitation in porous
7 medium and consequently the reservoir permeability does not decrease. In addition, the
8 simultaneous injection of CO_2 and nano-fluid is more sufficient than the cyclic injection. **Also,**
9 **Karambeygi et al., (2016) indicated that the salicylic acid can inhibit the asphaltene precipitation.**
10 **In addition, the high polar/aromatic inhibitors are similar to natural state of the resins which can**
11 **keep asphaltene particles in solution.** **Joonaki et al., (2017) investigated the asphaltene**
12 **precipitation using a quartz crystal microbalance technique to provide the most suitable scenario**
13 **for injection of commercial inhibitors/solvent at field conditions. Their results illustrated that the**
14 **reservoir conditions (pressure and temperature) and presence of gas might change the ranking of**
15 **commercial inhibitors for reducing the asphaltene precipitation.** Consequently, the conventional
16 treatment of asphaltene precipitation/deposition is categorized into two methods during gas
17 injection: (a) the liquid-based chemical was added to the crude oil samples as asphaltene
18 inhibitors and (b) the gas alternating chemical solution (inhibitors) injection into the reservoir.
19 The first case is not applicable in the field scale and just illustrates the performance of the
20 inhibitor on asphaltene stabilization in crude oils. Also, the second scenario can be used in field-
21 scale, but it involves three-phase flow. Three-phase displacement (oil, gas, and chemical
22 solution) can be provided with some limitation during gas injection. The process is highly
23 affected by gravity at higher gas mobility and the gas/chemical solution gravity segregation can

1 play a negative role in this process. However, in our previous work ([Azizkhani and Gandomkar,](#)
2 [2020](#)), liquid-free chemicals have been used as direct asphaltene inhibitors through CO₂ injection
3 for the first time. This method involves two-phase flow displacement along with the inhibitor.
4 Based on our previous work, the metal oxide nanoparticles (Fe₃O₄ and Al₂O₃) were considered
5 as inhibitors while CO₂ injection. Subsequently, the asphaltene stabilization through
6 CO₂/nanoparticles injection was investigated using static precipitation tests for **two different live**
7 **oil samples**, i.e., volatile and intermediate live oil. Furthermore, it was noted that the amount of
8 asphaltene precipitation was mitigated when CO₂/nanoparticles was injected compared to the
9 case when pure CO₂ was injected. In addition, the mixtures that contain Fe₃O₄ could perform
10 better than Al₂O₃ solutions; therefore the impact of solubility is more dominant than the effect of
11 the aggregation during the injection of DAI. However, this study focused on asphaltene
12 deposition in carbonate reservoir cores by analyses of dynamic asphaltene tests. Four metal oxide
13 nanoparticles such as GO, TiO₂, SiO₂, and MgO were used as DAIs for asphaltene precipitation
14 to make the asphaltene more stable in the insitu oil sample during the injection of the carbon
15 dioxide. The cloud point pressure was monitored to ensure that the mixture of CO₂/nanoparticles
16 is single-phase. Once the impact of DAIs was studied on asphaltene deposition at the reservoir
17 conditions by static and dynamic asphaltene tests. This study considered a new approach for the
18 application of inhibitors in porous media during gas injection. This method can be performed for
19 other asphaltene inhibitors (alkaline and surfactant-based chemicals) as direct asphaltene
20 inhibitors.

21 **2. Materials and methods**

22 • **Direct asphaltene inhibitors (DAI)**

1 Four metal oxide nanoparticles such as the graphene oxide (GO, MW = 12.01 gr/mol), titanium
2 dioxide (TiO₂, MW = 79.87 gr/mol), silicon dioxide (SiO₂, MW = 60.08 gr/mol), and
3 magnesium oxide (MgO, MW = 40.3 gr/mol) were used as direct inhibitor agents to make the
4 asphaltene more stable in the reservoir live oil during the immiscible/miscible carbon dioxide
5 injection. The metal oxide nano-particles generally have acidic, basic or amphoteric chemical
6 characteristics, which causes polar interactions between asphaltenes molecules and nano-
7 particles. However, the chemical nature of metal oxide nanoparticles considered in this study is
8 acidic (SiO₂ and TiO₂) and basic (MgO and GO) (Nassar et al., 2011; Dai et al., 2014). All the
9 inhibitors are commercially available and were used in the experiment as they were received.
10 Different concentrations of nanoparticles were used in this study, i.e. 50, 100, 200, and 300 ppm
11 for GO and 500, 1000, 2000, and 3000 ppm for other DAIs. The SARA (Saturates, Aromatics,
12 Resins and Asphaltenes) analysis of reservoir crude oil with °API of 23.65 was reported in **Table**
13 **1**. The colloidal instability index (CII) was considered to investigate the instability of the crude
14 oil. It should be noted that the CII is an index which highlights the ratio of asphaltene and
15 saturate summation to the summation of resins and aromatics. If the CII value of a crude oil
16 sample is greater than 0.9, the crude oil is expressed as unstable (Ghloum et al., 2010 and 2019).
17 However, according to SARA data, the CII value for reservoir crude oils is 1.60, and it
18 demonstrates the asphaltene precipitation possibilities for these cases. However, in this work, the
19 recombined live oil was used in the experiments to study the asphaltene deposition at the
20 reservoir conditions. The results of a constant composition expansion (CCE) experiment were
21 used to guarantee that the recombined oil could represent the in-situ reservoir fluid with
22 acceptable accuracy. The CCE result illustrates that the measured bubble point pressure is

1 consistent with the real reservoir oil bubble point pressure (Gandomkar et al., 2012). The
2 reservoir pressure and temperature are 3150 psia and 60 °C, respectively.

3 **Table 1**

4 **• Cloud point pressure measurements**

5 The authors considered liquid-free additives as DAIs throughout CO₂ injection at the reservoir
6 conditions. The dissolution of DAIs (GO, TiO₂, SiO₂, and MgO) in CO₂ was investigated by
7 calculation of cloud point pressures. The cloud point appears the pressure at which cloudiness in the
8 solution is first observed as the pressure is lowered. It was measured by HPHT visual cell with
9 different concentrations based on our previous work (Azizkhani and Gandomkar, 2020). At first,
10 a determined amount of DAI is weighed out and insert into the window cell. After that, a
11 specified amount of CO₂ was added to the sample to provide the desired composition. The
12 mixture with constant total composition was pressurized and then used a magnetic stirrer to
13 create a rotating magnetic field (2000 rpm). It was continued to achieve single-phase solutions
14 from the window cell at favorable temperatures and pressures. Finally, the reduction in pressure
15 of all samples was considered at the intervals of 40 psi. The equilibrium condition took about
16 two hours to identify any visual changes. Also more time might be needed for the low solubility
17 materials. In general, the cloud point pressures of DAI/CO₂ were indicated in the fog form by
18 visual monitoring in the bulk sample (Miller et al., 2009; Lee et al., 2016). The measurements
19 were repeated at least three times with reproducibility of ±5 psi. Subsequently, these mixtures
20 were considered in all experiments to certify that the single-phase solution has occurred.
21
22
23

1 • **Minimum miscibility pressure (MMP)**

2 The IFT measurements between the live oil and DAI/CO₂ were performed by the high-pressure
3 high-temperature IFT 700 apparatus. All the mixtures of hydrocarbon gas and DAIs were
4 provided and then used to measure the IFTs at reservoir conditions (i.e. 3150 psia and 60 °C). An
5 oil droplet is produced from the end of the capillary needle, which surrounded by pure CO₂ or
6 DAI/CO₂ at required conditions. However, the IFTs were measured using advanced drop shape
7 analysis software. In addition, the IFT error calculated via the standard deviation of 4 repeated
8 measurements of each mix, and it was about ± 0.1. Also, the MMP measurement was conducted
9 using vanishing interfacial tension (VIT) procedure ([Azizkhani and Gandomkar, 2020](#); [Ghorbani
10 et al., 2014](#)).

11 • **Asphaltene precipitation, Static test**

12 To investigate the asphaltene precipitation throughout the injection of CO₂ and CO₂/DAI, the
13 PVT analysis was conducted. The PVT apparatus that was used in this study consisted the
14 followings: PVT cell, transfer container, back pressure regulation, air bath, HPLC pump,
15 sampling vessel, filter, recombination cell, and shaker. In the experiment, a certain volume of the
16 CO₂/DAI mixture was injected into the PVT cell that contained live oil at the reservoir
17 conditions. Next, the PVT cell was shaken for 24 hours at a chosen temperature and pressure.
18 Then, the mixture of the CO₂/DAI and live oil was then retained in a stationary position for
19 another day to ensure that the asphaltene precipitation was occurring. The crude oil sampling is
20 taken out for analysis of asphaltene precipitation during CO₂/DAI injection. High-pressure
21 filtration was used to separate the precipitated asphaltene from the oil at a constant pressure
22 during its displacement from the PVT cell into the sampling vessel. Subsequently, the IP 143

1 standard method was conducted to measure the amount of the asphaltene content of the sample
2 for all CO₂/DAI mixtures (Azizkhani and Gandomkar, 2020; Arciniegas et al., 2014).

3 • **Asphaltene deposition, Dynamic test**

4 In order to study the impact of DAIs on the asphaltene precipitation and its deposition, a series of
5 coreflooding experiments were conducted during immiscible/miscible injection of CO₂. Full
6 details of the coreflooding process, the core flood apparatus and its components are provided
7 elsewhere (Gandomkar et al., 2015). To understand the impact of DAIs on asphaltene
8 precipitation and its subsequent deposition, the miscible CO₂/DAIs was injected into carbonate
9 core samples with the initial water and oil saturations similar to those of the initial reservoir
10 conditions. In the course of the core flood experiments, the produced oil was gathered to measure
11 the asphaltene deposition into the carbonate cores. To accurately determine the asphaltene
12 content in the produced oil using spectrophotometry, a minimum of one gram of produced oil
13 sample was required (Nguele et al., 2016; Srivastava et al., 1999; Li et al., 2018). The CO₂
14 injection was conducted up to two pore volumes with a frontal advance rate of 0.1 cm³/min.
15 Also, the scaling criterion of Rappaport and Leas (1953) has been considered to remove the
16 dependence of oil recovery factor on core length and gas injection rate due to capillary end
17 effect. It should be noted that the amount of asphaltene deposition was estimated by subtraction
18 of the asphaltene content of the original crude oil from that of the produced oil. The amount of
19 asphaltene deposition divided by initial asphaltene content and has been reported as a
20 dimensionless parameter. The properties of carbonate cores were reported in Table 2. The
21 average porosity and permeability ranged between 13 to 16 percent and 7 to 9 md, respectively
22 (Cao et al., 2013).

23 **Table 2**

1 **3. Results and discussion**

2 The effect of GO, TiO₂, SiO₂, and MgO, as direct asphaltene inhibitors, on asphaltene
3 precipitation and deposition was studied during miscible CO₂ injection. The SARA analysis and
4 CII values were conducted to show the asphaltene precipitation possibilities for these cases.
5 Besides, the cloud point pressure of all the CO₂/nanoparticles mixtures was measured to ensure
6 that the single-phase conditions have occurred during asphaltene precipitation tests. Also, the
7 asphaltene precipitation and deposition investigated by static and dynamic tests, respectively at
8 reservoir conditions (i.e. 60 °C and 3150 psia).

9 • **Phase behavior of DAI/CO₂ by cloud point pressure measurements**

10 In **Table 3**, the cloud point pressures of CO₂ mixtures with GO, TiO₂, SiO₂, and MgO for
11 different temperatures of 25, 40, 60, and 80 °C is listed. It should be noted that, throughout cloud
12 point pressure measurements, the concentration of nano-particles were ranging from 50 to 300
13 ppm for GO and 500 to 3000 ppm for others. The cloud point pressures were ranging from 1400
14 to nearly 2500 psia. The cloud point pressure normally rises as the concentration of nano-
15 particles in the solution increases. Additionally, the cloud point pressures increase almost
16 linearly with increase in temperature. e.g., the cloud point pressures of GO illustrated that the
17 dissolution of direct asphaltene inhibitor in CO₂ has occurred at 1712, 1830, 1994, and 2159 psia
18 in different concentration; 50, 100, 200, and 300 ppm; respectively at reservoir temperature (i.e.
19 60 °C). According to these observations, all the cloud point pressures are lower than reservoir
20 pressure and consequently, the single-phase conditions occur during asphaltene
21 precipitation/deposition tests for all direct asphaltene inhibitors. The effect of temperature on the
22 cloud point pressure of CO₂/DAI is shown in **Figure 1** at different concentrations. Additionally,
23 the solubility of DAIs increase as the temperature decreases. This observation highlights that the

1 density is directly proportional to the solubility. It could be explained by the entropy of mixing
2 and its dependency to the temperature. The density of CO₂ reduces significantly at higher
3 temperatures, whereas the impact of temperature on the nanoparticles density is minimal. If the
4 density of CO₂ becomes significantly different from that of nanoparticles, the entropy of mixing
5 becomes negative and then the temperature has a converse impact on the system (Joung et al.,
6 2002). Based on these results, the cloud point pressures of GO are lower than other nanoparticles
7 considered in this study at the same temperature. The molecular weights of nanoparticles have an
8 impact on the solubility in CO₂, this is due to entropic impacts and coupled with the unwanted
9 enthalpy interactions related to the CO₂-phobic functionalities and CO₂ (Yu et al., 2014; Chu et
10 al., 2019). As it was observed, all the DAIs/CO₂ mixtures were single-phase at reservoir
11 conditions and then these solutions were used for all asphaltene precipitation experiments.

12 **Table 3**

13 **Figure 1**

14 **• MMP measurements**

15 The amount of asphaltene precipitation will be different during miscible and immiscible CO₂
16 injection. Cao et al., (2013) illustrated that the miscible CO₂ injection causes more asphaltene
17 precipitation compared to immiscible injection. However, in this study, vanishing interfacial
18 tension technique was used to investigate the effect of DAI on MMP. At first, at equilibrium
19 pressures ranging from 2500 to 3150 psia, the interfacial tension between live oil and pure/DAIs
20 CO₂ were assessed. It should be noted that all the IFT values were measured at the reservoir
21 temperature and pressures higher than the cloud point pressure to make sure that the mixtures of
22 the CO₂/Nanoparticles are single phase. In Table 4, the results of live oil-pure CO₂ and

1 DAI_s/CO₂ mixtures at T_{res}= 60 °C are listed. Considering the data of **Table 4**, the IFT for pure
2 CO₂, 200 ppm GO, 2000 ppm TiO₂, 2000 ppm SiO₂, and 2000 ppm MgO are 46, 13, 15, 14, and
3 15 dyne/cm, **respectively** at 2500 psia and 60 °C. The asphaltenes are known to be one of the
4 most surface-active compounds in crude oil and could be absorbed to the DAI_s surface and
5 reduce the IFTs. The metal oxide (DAI_s) surface will typically have high surface energy. It was
6 noted that GO could expressively decrease IFT compared to other DAI_s considered in this study.
7 It referred to the high specific surface area of GO compared to other DAI_s. In addition, an
8 increase in equilibrium pressure led to a significant reduction in IFT. It is well understood that as
9 the IFT between live oil and nanoparticles/carbon dioxide decreases it will increase the
10 miscibility and subsequently leads to a decrease in the residual oil saturation ([Ghorbani et al.,
11 2014](#)). As shown in [Figure 2](#), it is noted that MMP decreases as the concentration of the
12 nanoparticles increases. It is due to the fact that the density of the mixture of the nanoparticles
13 and CO₂ is slightly larger than the pure carbon-dioxide; this leads to a lower difference in density
14 with that of the live oil and therefore smaller IFT values than pure carbon-dioxide ([Chu et al.,
15 2019](#)). It is also shown that the MMP for GO/CO₂ is lower than that of the other mixtures. The
16 MMPs are 3370, 2941, 3006, 2938, and 3040 psia for pure CO₂, 200 ppm GO, 2000 ppm TiO₂,
17 2000 ppm SiO₂, and 2000 ppm MgO, **respectively** at reservoir temperature, 60 °C. Hence, the
18 MMP for pure CO₂ is above the P_{res}=3150 psi; and consequently, the immiscible conditions will
19 occur during pure CO₂ injection for asphaltene precipitation/deposition tests. Furthermore, the
20 MMPs for all CO₂/DAI_s are smaller than reservoir pressure, and as a result, miscible conditions
21 occur during static and dynamic asphaltene processes.

22 **Table 4**

23 [Figure 2](#)

1 • **PVT analysis of asphaltene precipitation through CO₂/DAI injection**

2 In this work, the team used nanoparticles as direct asphaltene inhibition agent to prevent the
3 asphaltene precipitation by static test during CO₂ injection. In all experiments, to guarantee that
4 all solutions are single-phase, the mixtures of CO₂/nanoparticles were injected at a pressure
5 higher than the cloud point pressure. The live oil has 6.4 weight percent initial asphaltene content
6 and from **Table 5**, the amounts of 5.8 weight percent asphaltene precipitated during pure
7 immiscible injection of CO₂. It was expected that the amount of asphaltene precipitation
8 increases during miscible DAIs/CO₂ but it reduced using nanoparticles as direct asphaltene
9 inhibitors. The amount of asphaltene precipitation reduced from 5.8 to 3.1, 4.2, 4, and 3.8 weight
10 percent by using 100 ppm GO, 1000 ppm TiO₂, 1000 SiO₂, and 1000 ppm MgO mixtures,
11 **respectively**. Additionally, the CO₂/GO mixtures decreased the amounts of asphaltene
12 precipitation higher than other DAIs considered in this study. The specific surface area of the GO
13 (890 m²/g) is higher than that for TiO₂ (174.5 m²/g), SiO₂ (590 m²/g), and MgO (300 m²/g);
14 consequently, it led to more adsorption of asphaltene (Yu et al., 2014; Karambeygi et al., 2016;
15 Chu et al., 2019). The application of nanoparticles could enhance the solubility of asphaltene in
16 the live oil and consequently lead to a reduction in the precipitation of asphaltene. Likewise, it
17 increases the CO₂ solubility, dilutes the live oil, subsequently disperses the resin molecules, and
18 finally leads to asphaltene stabilization in oil. Also, the amounts of asphaltene precipitation
19 decreased by increasing DAI concentrations. The lone pair electrons, i.e., a pair of valence
20 electrons, of oxygen intensify the surface negative charge density of the metal oxide
21 nanoparticles, which enhances the adsorption of asphaltene fraction. It should be noted that there
22 is an insignificant reduction in asphaltene precipitation for the duration of a high concentration of
23 DAIs. For example, the **amounts** of asphaltene precipitation are 2.5 and 2.4 weight percent for

1 200 and 300 ppm GO, respectively. For that reason, the DAI concentration of 200 ppm can be
2 more efficient than other DAI concentrations through miscible CO₂/GO injection. It was
3 previously reported that the optimal concentration for Fe₃O₄ and TiO₂ nanoparticles in the
4 inhibitor is approximately one weight percent (Hassanpour et al., 2018). In addition, it will
5 decrease the asphaltene precipitation to seventeen and eighteen percent of initial content of
6 asphaltene using TiO₂ and Fe₃O₄ correspondingly. When a low concentration of inhibitor is
7 applied, active site on the structure of asphaltene could be occupied by free monomers and
8 consequently stabilizes the asphaltene particles within the solution (Rocha et al., 2006).
9 Additionally, the polar head group of the inhibitor has a dissimilar potential to attach to the
10 particles and makes the system of the inhibitor/asphaltene more stable. It should be highlighted
11 that these groups' polarity governs the strength of the bond. However, when a high concentration
12 of inhibitors is used, it will not lead to the desired result. As the inhibitors' concentration rises,
13 the likelihood of self-association under hydrogenous bonding increases accordingly. Conversely,
14 when a higher concentration of inhibitor is applied, the potential of self-association in inhibitor-
15 inhibitor is larger than the inhibitor/asphaltene's interaction. Consequently, the capability of
16 inhibitors on the stabilization of the asphaltenes decreases and it will cause the inhibitors to
17 underperform at higher concentrations (Karambeygi, 2016; Leon et al., 2001). As a result, the
18 metal oxide nanoparticles have acidic/basic/amphoteric chemical characteristic, which causes
19 polar interactions between asphaltenes particles and nanoparticles. The bond formation between
20 nanoparticles (metal oxide) and asphaltene particles is a key factor that delays the beginning
21 point of separation of asphaltenes from oil, i.e., onset. The asphaltene particles could be
22 suspended in resins due to the formation bonding of metal-oxide nanoparticles and asphaltene
23 molecules and its bonding to the activated sites on the surface of the asphaltene particles (Nassar

1 et al., 2011). It should be noted there are two conflicting forces affecting the precipitation, i.e.,
2 aggregation effect and the solubility mechanism. The first force (aggregation effect) has a
3 tendency to lead to precipitation whilst the second (solubility mechanism) tends to retain the
4 asphaltene molecules in the solution. Furthermore, the results show that the impact of the
5 solubility mechanism is more dominant than that of the aggregation effect for the duration of the
6 injection of CO₂/nanoparticles (Gharbi et al., 2017; Rashid et al., 2019; Yen et al., 2001).

7 **Table 5**

8 **• The effect of DAI on asphaltene deposition**

9 The amount of asphaltene deposition into the carbonate cores was measured during coreflooding
10 tests for pure and CO₂/DAIs injection. Figure 3 shows the variation in the asphaltene content of
11 the produced oil with injected PV of pure and CO₂/DAIs injection during carbonate cores. The
12 asphaltene concentration in the oil was constant till CO₂ breakthrough which occurred at around
13 0.25 pore volumes (PV) and 0.35 PV for pure CO₂ and CO₂/DAIs mixtures, respectively.

14 Because the produced oil had not yet been in contact with the injected pure CO₂ and CO₂/DAIs,
15 the change in asphaltene content was insignificant. Inversely, the asphaltene content in the
16 produced oil after the CO₂ breakthrough reduced significantly. The drop in asphaltene content
17 highlights the fact that some further asphaltene precipitation/flocculation occurs in the carbonate
18 cores during pure and CO₂/DAIs injection. From Figure 3, the asphaltene content in produced oil
19 during injection of DAIs/CO₂ mixtures are higher than that for pure CO₂ injection. It shows that
20 the metal oxide nanoparticles can stabilize the asphaltene particles in reservoir oil. In addition,
21 the mixture of GO/CO₂ improved the asphaltene stabilization compared to other DAIs
22 considered in this study. From this result, the amount of asphaltene content in produced oil are
23 1.3, 5.4, 4.1, 3, and 5 weight percent after injection of 2 PV pure CO₂, 200 ppm GO, 2000 ppm

1 SiO₂, 2000 TiO₂, and 2000 ppm MgO mixtures, respectively. Also, Figure 4 illustrates the
2 amount of asphaltene's deposition in the carbonate cores by the subtraction of the asphaltene
3 content in the produced oil from that of the initial crude oil during the dynamic tests. The amount
4 of asphaltene deposition significantly decreased during injection of CO₂/DAIs mixtures
5 compared to pure CO₂ injection. The metal oxide nanoparticles hinder the phase separation of
6 asphaltenes kinetically and prevent growth. It is conducted by stabilizing the colloidal
7 suspension of the asphaltene particles, which are in sub-micrometer size to significantly slow the
8 asphaltene flocculation onset. Consequently, the direct asphaltene inhibitors can prevent to
9 asphaltene deposition and act as asphaltene dispersants. The polyaromatic nuclei with aliphatic
10 side chains and rings of asphaltene connect and create micellar aggregates. This is well-
11 documented that in addition to aromatic compounds, asphaltenes consist of different acidic and
12 basic functional groups. The metal oxide nanoparticles that are adsorbed on the micelle core
13 make the asphaltene micelles more stable. The DAIs connects to the asphaltene particles using
14 their polar head and expands their aliphatic group outward. This creates a layer round
15 asphaltenes. On the condition that the asphaltene particles are stabilized in the micelles,
16 precipitation does not occur (Setaro et al., 2019).

17 **Figure 3**

18 **Figure 4**

19 Besides, using asphaltene particle size analysis approach, the team measured the mean size of the
20 asphaltene particles to study the impact of direct asphaltene inhibitors on asphaltene particle size
21 for the duration of pure CO₂ injection and 200 ppm GO/CO₂ mixture injection, Figures 5 and 6.
22 Based on this result, the asphaltene particle size during pure CO₂ injection is higher than that for
23 GO/CO₂ mixture injection. It is clear that the GO/CO₂ mixtures can stabilize the asphaltene

1 particles in oil and significantly reduces the size of asphaltene particles simultaneously. The total
2 size of asphaltene particles which precipitated during the injection of pure CO₂ and 200 ppm
3 GO/CO₂ mixture are 2657808 and 756592 μm², respectively. The particles are created in two
4 different stages, i.e., phase separation stage and asphaltene particle growth stage. Phase
5 separation takes place when asphaltene particles in the oil precipitate and develop into large
6 aggregates. Additionally, the stability of asphaltene particles can be improved by the introduction
7 of compounds, which hold a polar head containing an acidic group, which can attach to the
8 micellar core. Dissimilar acidities are observed for amphiphiles with diverse head groups. The
9 inhibition capability of amphiphiles depends on the fact that how strong are their groups' acidity,
10 therefore the amphiphiles stabilize the asphaltene in the solution via the acid-base interaction.
11 The ability of amphiphiles' inhibition is related to the strength of these groups acidity and
12 illustrating that the asphaltene stabilization occurs through the acid-base interaction (Zanganeh et
13 al., 2018). However, direct asphaltene inhibitors can decrease the amount of asphaltene
14 precipitation and also prevents the aggregation of precipitated asphaltene particles. By the way,
15 the size of deposited asphaltene particles can affect the oil flow in porous media due to changing
16 the pressure drop. Based on the dynamic tests, the differential pressure during the pure CO₂
17 injection was higher than that for injection of CO₂/DAIs mixtures. It referred to asphaltene
18 precipitation, which increased formation damage during the pure CO₂ injection compared to
19 other cases. Figure 7 shows the schematic of asphaltene deposition on the rock surface. The
20 asphaltenes may adsorb onto the rock surface and cause permeability blockage, wettability
21 alteration to oil-wet, reduces the oil effective permeability; and thereby decreases the oil
22 recovery (Figure 7a). However, the application of direct asphaltene inhibitors can stabilize the
23 asphaltene particles and also prevent to asphaltene deposition as a dispersant (Figure 7b).

1 Additionally, the presence of the metal oxide nanoparticles as direct asphaltene inhibitors can
2 enhance the **oil recovery factor between 6 to 25** percent compared to pure CO₂ injection. The
3 adsorption performance of asphaltenes on the metal oxide nanoparticles is governed by two
4 properties, i.e., the surface energy and the structure of nanoparticles and the chemical and
5 physical characteristics of the asphaltene particles and polar, electrostatic, and van der Waals
6 interactions are the key factors which influence the asphaltene adsorption onto the solid surfaces.
7 Among these three factors, the acid–base (polar) and electrostatic interaction are the most
8 significant factors. It is well-documented that surface Gibbs energy reduced by the adsorption of
9 asphaltene particles on the nanoparticles. Consequently, the nanoparticles containing asphaltene
10 (which are adsorbed onto the surface of nanoparticles) have a weaker interaction compared to
11 those of the nanoparticles lacking asphaltene particles. Hence, the adsorbed asphaltene particles
12 onto the nanoparticles have higher stability in the reservoir rock ([Hosseinpour et al., 2013](#);
13 [Castro et al., 2009](#)). Throughout the CO₂/DAIs injection, the nanoparticles adsorb the
14 precipitated asphaltene particles and consequently alleviate the rate of the adsorption of
15 precipitated asphaltenes onto the rock surface and consequent deposition in the porous medium.
16 For that reason, the nanoparticles carrying asphaltenes could travel within the porous medium
17 and subsequently lead to inhibit the precipitation and as a result, prevents permeability reduction
18 due to asphaltene precipitation.

19 **Figure 5**

20 **Figure 6**

21 **Figure 7**

22

1 **4. Conclusions**

- 2 • Liquid-free inhibitors can be directly applicable for gas-based enhanced oil recovery in
3 field scale.
- 4 • The metal oxide nanoparticles could increase the stability of the colloidal asphaltenes and
5 consequently diminish the growing and the formation of flocculated asphaltene particles.
- 6 • The total size of asphaltene particles, which precipitated during injection CO₂/DAIs
7 mixture, is significantly lower than that for pure CO₂ injection.
- 8 • The effectiveness of the graphene oxide nanoparticle is much better than other DAIs in
9 retaining the asphaltene particles suspended and spread within the oil.
- 10 • The application of CO₂/GO mixtures could reduce the asphaltene aggregation/deposition
11 and improved the oil recovery factor between 6 to 25 percent compared to the case that
12 only CO₂ was injected.
- 13 • The cloud point pressure of CO₂/DAIs mixtures is under the reservoir pressure to certify
14 that the single-phase solution has occurred at reservoir conditions.
- 15 • The direct asphaltene inhibitors lead to a decrease in the IFT and provide the miscible
16 injection of gas at reservoir pressure and temperature.
- 17 • The metal oxide nanoparticles improved the solubility of the asphaltene particles and
18 consequently kept them in the solution.

19
20
21
22
23

- 1 **Nomenclature**
- 2 Colloidal Instability Index, CII
- 3 Constant Composition Expansion, CCE
- 4 Cubic Plus Association Equation of state, CPA
- 5 Deasphalted Crude Oil, DO
- 6 Direct Asphaltene Inhibitor, DAI
- 7 Dodecyl Benzene Sulfonic Acid, DDBSA
- 8 Dodecyl Risolsinol, DR
- 9 Graphene Oxide, GO
- 10 High-Pressure High-Temperature, HPHT
- 11 Liquefied Petroleum Gas, LPG
- 12 Magnesium Oxide, MgO
- 13 Minimum Miscibility Pressure, MMP
- 14 Nonyl Phenol, NP
- 15 Pressure, Volume, Temperature, PVT
- 16 Resins, R
- 17 Saturates, Aromatics, Resins, and Asphaltenes, SARA
- 18 Silicon Dioxide, SiO₂
- 19 Titanium Dioxide, TiO₂
- 20 Toluene, T
- 21 Vanishing Interfacial Tension, VIT
- 22 Weight percent, wt
- 23

1 **References**

2 Arciniegas, L.M., Babadagli, T., Asphaltene precipitation, flocculation and deposition
3 during solvent injection at elevated temperatures for heavy oil recovery, Fuel Journal, 124, 202-
4 211, 2014.

5 Azizkhani A., Gandomkar, A., A novel method for application of nanoparticles as direct
6 asphaltene inhibitors during miscible CO₂ injection, Journal of Petroleum Science and
7 Engineering, 185, 106661, 2020.

8 Bae, J., Fouchard, D., Garner, S., Macias, J., Advantages of Applying a Multifaceted
9 Approach to Asphaltene Inhibitor Selection, OTC 27171, 2016.

10 Cao, M., Gu, Y., Oil recovery mechanisms and asphaltene precipitation phenomenon in
11 immiscible and miscible CO₂ flooding processes, Fuel Journal, 109, 157-166, 2013.

12 Castro, M., Cruz, J.L., Ramirez, S., Villegas, A., Predicting adsorption isotherms of
13 asphaltenes in porous materials, Fluid Phase Equilibria, 286, 113-119, 2009.

14 Chu, T.M., Nguyen, N.T., Vu, T.L., Pham, T.D., Synthesis, Characterization, and
15 Modification of Alumina Nanoparticles for Cationic Dye Removal, Materials, 12, 450, 1-15,
16 2019.

17 Dai, J.F., Wang, G.J., Wu, Ch., Investigation of the Surface Properties of Graphene
18 Oxide and Graphene by Inverse Gas Chromatography, Chromatographia journal, 77, 299-307,
19 2014.

1 Gandomkar, A., Kharrat, R., Tertiary FAWAG Process on Gas and Water Invaded Zones,
2 an Experimental Study, Journal of Energy Sources, Part A: Recovery, Utilization, and
3 Environmental Effects, 34, 1913-1922, 2012.

4 Gandomkar, A., Rahimpour, M.R., Investigation of low salinity waterflooding in
5 secondary and tertiary enhanced oil recovery in limestone reservoirs, Energy & Fuels Journal,
6 29, 7781-7792, 2015.

7 Gharbi, Kh., Benyounes, Kh., Khodja, M., Removal and prevention of asphaltene
8 deposition during oil production: A literature review, Journal of Petroleum Science and
9 Engineering, 158, 351-360, 2017.

10 Ghloum, E.F., Qahtani, M.A., Rashid, A., Effect of inhibitors on asphaltene precipitation
11 for Marrat Kuwaiti reservoirs, Journal of Petroleum Science and Engineering, 70, 99-106, 2010.

12 Ghloum, E.F., Rashed, A.M., Safa, M.A., Mitigation of asphaltenes precipitation
13 phenomenon via chemical inhibitors, Journal of Petroleum Science and Engineering, 175, 495-
14 507, 2019.

15 Ghorbani, M., Momeni, ., Safavi, S., Gandomkar, A., Modified Vanishing Interfacial
16 Tension (VIT) Test for CO₂-Oil Minimum Miscibility Pressure (MMP) Measurement, Journal of
17 Natural Gas Science and Engineering, 20, 92-98, 2014.

18 Hassanpour, S., Malayeri, M.R., Riazi, M., Utilization of CO₃O₄ nanoparticles for
19 reducing precipitation of asphaltene during CO₂ injection, Journal of Natural Gas Science and
20 Engineering, 31, 39-47, 2016.

1 Hassanpour, S., Malayeri, M.R., Riazi, M., Asphaltene Precipitation during Injection of
2 CO₂ Gas into a Synthetic Oil in the Presence of Fe₃O₄ and TiO₂ Nanoparticles, Journal of
3 chemical engineering data, 63 (5), 1266-1274, 2018.

4 Hong, E., Watkinson, P., A study of asphaltene solubility and precipitation. Fuel journal,
5 83, 1881-1887, 2004.

6 Hosseinpour, N., Khodadadi, A.A., Bahramian, A., Mortazavi, Y., Asphaltene adsorption
7 onto acidic/basic metal oxide nanoparticles toward in situ upgrading of reservoir oils by
8 nanotechnology, Langmuir, 29, 14135-14146, 2013.

9 Hu, Y.F., Guo, T.M., Effect of the structures of ionic liquids and alkylbenzenederived
10 amphiphiles on the inhibition of asphaltene precipitation from CO₂-injected reservoir oils,
11 Langmuir, 21, 8168-8174, 2005.

12 Ibrahim, H.H., Idem, R.O., Inter relationships between Asphaltene Precipitation Inhibitor
13 Effectiveness, Asphaltenes Characteristics, and Precipitation Behavior during n-Heptane (Light
14 Paraffin Hydrocarbon) -Induced Asphaltene Precipitation, Energy & Fuels, 18, 1038-1048, 2004.

15 Joonaki, E., Burgass, R., Hassanpouryouzband, A., Tohidi, B., Comparison of
16 experimental techniques for evaluation of chemistries against asphaltene aggregation and
17 deposition: new application of high-pressure and high-temperature quartz, Energy & Fuels, 32, 3,
18 2712-2721, 2017.

19 Joonaki, E., Buckman, J., Burgass, R., Tohidi, B., Water versus Asphaltenes; Liquid-
20 Liquid and Solid-Liquid Molecular Interactions Unravel the Mechanisms behind an Improved
21 Oil Recovery Methodology, Scientific Reports, 9, 1, 11369, 2019.

1 Joonaki, E., Hassanpouryouzband, A., Burgass, R., Hase, A., Tohidi, B., Effects of
2 Waxes and the Related Chemicals on Asphaltene Aggregation and Deposition Phenomena:
3 Experimental and Modeling Studies, ACS omega 5, 13, 7124-7134, 2020.

4 Joung, S.N., Park, J.U., Kim, S.Y., High-pressure phase behavior of polymersolvent
5 systems with addition of supercritical CO₂ at temperatures from 323.15 K to 503.15 K,
6 Journal of Chemical & Engineering Data, 47, 2, 270-273, 2002.

7 Karambeygi, M.A., Nikazar, M., Kharrat, R., Experimental evaluation of asphaltene
8 inhibitors selection for standard and reservoir conditions, Journal of Petroleum Science and
9 Engineering, 13, 74-86, 2016.

10 Kazemzadeh, Y., Malayeri, M.R., Riazi, M., Parsaei, R., Impact of Fe₃O₄ nanoparticles
11 on asphaltene precipitation during CO₂ injection, Journal of Natural Gas Science and
12 Engineering, 22, 227-234, 2015.

13 Kelland, M.A., Asphaltene control. Production Chemicals for the Oil and Gas Industry.
14 Stavanger, Norway: University of Stavanger, Chapter 4, 2009.

15 Leonard, G.Ch., Ponnappati, R., Rivers, G., Novel Asphaltene Inhibitor for Direct
16 Application to Reservoir, SPE 167294, 2013.

17 Leon, O., Contreras, E., Rogel, E., Dambakli, G., Espidel, J., Avedo, S., The influence
18 of the adsorption of amphiphiles and resins in controlling asphaltene flocculation, Energy and
19 Fuels, 15, 102-1032, 2001.

20 Lee, J.J., Dhuwe, A., Stephen, D., Eric, J., Enick, R.M., Polymeric and Small Molecule
21 Thickeners for CO₂, Ethane, Propane and Butane for Improved Mobility Control, SPE Improved
22 Oil Recovery Conference, Tulsa, SPE 179587, 2016.

1 Li, X., Guo, Y., Sun, Q., Lan, W., Guo, X., Experimental study for the impacts of flow
2 rate and concentration of asphaltene precipitant on dynamic asphaltene deposition in
3 microcapillary medium, *Journal of Petroleum Science and Engineering*, 162, 333-340, 2018.

4 Lu, T., Li, Zh., Fan, W., Zhang, X., Nanoparticles for Inhibition of Asphaltenes
5 Deposition during CO₂ Flooding, *Industrial & Engineering Chemistry Research*, 55 (23), 6723-
6 6733, 2016.

7 Miller, M.B., Chen, D.L., Xie, H.B., Luebke, D.R., Enick, R.M., Solubility of CO₂ in
8 CO₂-philic oligomers; cosmothem predictions and experimental results, fluid phase equilibria,
9 287, 26-32, 2009.

10 Nassar, N.N., Hassan, A., Pereira, A.P., Metal oxide nanoparticles for asphaltene
11 adsorption and oxidation, *Energy & Fuels*, 25, 3, 1017-1023, 2011.

12 Nguele, R., Ghulami, M.R., Sasaki, K., Asphaltene Aggregation in Crude Oils during
13 Supercritical Gas Injection, *Energy and Fuels*, 30, 2, 1266-1278, 2016.

14 Rappaport, L.A., Leas, W.J. 1953, "Properties of Linear Waterfloods, presented at the Fall Meeting of the
15 Petroleum Branch in Houston, Texas, SPE 213-G.

16 Rashid, Z., Wilfred, C.D., Murugesan, Th., A comprehensive review on the recent advances on
17 the petroleum asphaltene aggregation, *Journal of Petroleum Science and Engineering*, 176, 249-
18 268, 2019.

19 Reubush, S. D., Effects of storage on the linear viscoelastic response of polymer-
20 modified asphalt at intermediate to high temperatures, MS Thesis, Virginia Polytechnic Institute
21 and State University, Blacksburg, VA, 1999.

1 Rocha, L.C., Ferreira, M.S., Ramos, A.C., Inhibition of asphaltene precipitation in
2 Brazilian crude oils using new oil soluble amphiphiles, *Journal of Petroleum Science and*
3 *Engineering*, 51, 26-36, 2006.

4 Setaro, L.O., Pereira, V.J., Costa, G.M., Melo, S., A novel method to predict the risk of
5 asphaltene precipitation due to CO₂ displacement in oil reservoirs, *Journal of Petroleum Science*
6 *and Engineering*, 176, 1008-1017, 2019.

7 Shojaati, F., Riazi, M., Mousavi, S.H., Experimental investigation of the inhibitory
8 behavior of metal oxides nanoparticles on asphaltene precipitation, *Colloids and Surfaces A:*
9 *Physicochemical and Engineering Aspects*, 531, 99-110, 2017.

10 Srivastava, R.K., Huang, S.S., Dong, M., Asphaltene Deposition During CO₂ Flooding,
11 *SPE Production & Facilities*, SPE 59092, 14, 4, 1999.

12 Stephenson, W.K., *Producing Asphaltene Crude Oils: Problems and Solutions*, *Petroleum*
13 *Engineer*, 24, 1990.

14 Taher, A.S., Mohammed, A.F., Amal, S.E., Retardation of asphaltene precipitation by
15 addition of toluene, resins, deasphalted oil and surfactants, *Fluid Phase Equilibria* 194-197,
16 1045-1057, 2002.

17 Varamesh, A., Hosseinpour, N., Prediction of Asphaltene Precipitation in Reservoir
18 Model Oils in the Presence of Fe₃O₄ and NiO Nanoparticles by Cubic Plus Association
19 Equation of State, *Industrial & Engineering Chemistry Research*, 58 (10), 4293-4302, 2019.

20 Yen, A., Yin, Y.R., Asomaning, S., Evaluating Asphaltene Inhibitors: Laboratory Tests
21 and Field Studies, SPE 65376, 2001.

1 Yin, Y.R., Yen, A.T., Asphaltene Deposition and Chemical Control in CO₂ Floods, SPE-
2 59293, 2000.

3 Yu, H., Li, Y., Fan, L., Yang, Sh., Highly dispersible and charge-tunable magnetic
4 Fe₃O₄ nanoparticles: facile fabrication and reversible binding to GO for efficient removal of dye
5 pollutants, Journal of Materials Chemistry A, 38, 2, 15763-15767, 2014.

6 Zanganeh, P., Dashti, .H, Ayatollahi, Sh., Comparing the effects of CH₄, CO₂, and N₂
7 injection on asphaltene precipitation and deposition at reservoir condition: A visual and
8 modeling study, Fuel, 217, 633-641, 2018.

9
10
11
12
13
14
15
16
17
18
19
20
21
22
23

1 **List of Tables**

2 **Table 1:** Reservoir oil properties

3 **Table 2:** Carbonate rock properties

4 **Table 3:** Cloud point pressure (psia) of CO₂ and GO, TiO₂, SiO₂, and MgO nanoparticles
5 mixtures at different nanoparticle concentrations at 25, 40, 60, and 80 °C

6 **Table 4:** IFT measurements of pure CO₂ and CO₂/nanoparticles with reservoir oil, at different
7 DAI concentrations at reservoir temperature ($T_{res}= 60$ °C), and MMP of these mixtures which
8 measured by VIT technique

9 **Table 5:** The effect of GO, TiO₂, SiO₂, and MgO nanoparticles on asphaltene precipitation as
10 direct asphaltene inhibitors during static test at reservoir conditions, 60 °C and 3150 psia

11

12

13

14

15

16

17

18

19

20

21

22

23

24

1
2
3
4
5
6
7
8
9
10
11
12
13
14
15
16
17

Table 1

Reservoir oil properties	Values
Saturates	55.10 wt
Aromatics	22.90 wt
Resins	15.60 wt
Asphaltenes	6.40 wt
CII	1.60
API	23.65
Molecular weight, g/mol, IP-86	164.80
S.G (60°F), ASTM-D40452	0.91
Acid Number, mg/g (KOH)	1.45
T _{res} (°C)	60
P _{res} (psia)	3150

1
2
3
4
5
6
7
8
9
10
11
12
13
14
15
16
17
18
19
20

Table 2

Limestone Cores No.	Length (cm)	Diameter (in)	PV (cc)	Helium Porosity (Percent)	Permeability (mD)	Connate Water (Percent)
C1	7.5	1.5	11.9	13.91	7.5	27.9
C2	7.4	1.5	12.5	14.81	8.2	29.5
C3	7.7	1.5	13.3	15.15	8.6	28.4
C4	7.8	1.5	13.0	14.61	7.8	29.1
C5	7.7	1.5	13.1	14.92	8.3	28.5

1
2
3
4
5

6
7
8
9
10
11
12
13
14
15

Table 3

DAI	Concentration (ppm)	Cloud point pressure (psia)			
		25 °C	40 °C	60 °C	80 °C
GO	50	1419	1538	1712	1935
	100	1527	1659	1830	2061
	200	1670	1812	1994	2215
	300	1746	1971	2159	2406
TiO ₂	500	1631	1724	1921	2126
	1000	1731	1862	2026	2243
	2000	1865	2028	2183	2388
	3000	1953	2159	2340	2589
SiO ₂	500	1574	1663	1859	2080
	1000	1653	1725	1938	2180
	2000	1785	1947	2105	2300
	3000	1883	2082	2265	2497
MgO	500	1469	1575	1755	1971
	1000	1579	1690	1884	2118
	2000	1720	1882	2058	2263
	3000	1792	2046	2217	2483

1
2
3
4
5
6
7
8
9
10
11
12

Table 4

DAI	Concentration (ppm)	IFT (dyn/cm) Live oil/CO ₂ -DAI, T _{res} = 60 °C				
		P=2500 psia	P=2800 psia	P=3000 psia	P _{res} =3150 psia	MMP (psia)
GO	Pure CO ₂	46	31	20	12	3370
	50	28	16	7	0	3100
	100	18	9	1	0	3049
	200	13	4	0	0	2941
	300	6	0	0	0	2740
TiO ₂	500	34	19	8	0	3140
	1000	22	11	3	0	3115
	2000	15	6	1	0	3006
	3000	9	1	0	0	2811
SiO ₂	500	31	16	5	0	3115
	1000	20	10	1	0	3027
	2000	14	4	0	0	2938
	3000	7	0	0	0	2761
MgO	500	30	19	8	0	3110
	1000	19	11	2	0	3100
	2000	15	7	0	0	3040
	3000	8	1	0	0	2814

1
2
3
4
5

6
7
8
9
10
11
12
13
14

Table 5

DAI	Concentration (ppm)	Asphaltene Precipitation, Static Test (wt%)
	Pure CO ₂	5.8
GO	50	4.0
	100	3.1
	200	2.5
	300	2.4
TiO ₂	500	5.0
	1000	4.2
	2000	3.8
	3000	3.7
SiO ₂	500	4.8
	1000	4.0
	2000	3.5
	3000	3.4
MgO	500	4.5
	1000	3.8
	2000	3.5
	3000	3.5

1 **List of Figures**

2 **Figure 1:** The impact of temperatures (25, 40, 60, and 80 °C) on cloud point pressures of DAI
3 (GO, TiO₂, SiO₂, MgO) and CO₂

4 **Figure 2:** The effect of DAI on Minimum miscibility pressure measured by the VIT technique at
5 reservoir temperature, T_{res}= 60 °C

6 **Figure 3:** The impact of direct asphaltene inhibitors (GO, TiO₂, SiO₂, MgO) on asphaltene
7 content of the produced oil during dynamic tests at reservoir conditions, 60 °C and 3150 psia

8 **Figure 4:** The impact of direct asphaltene inhibitors (GO, TiO₂, SiO₂, MgO) on asphaltene
9 deposition during dynamic tests at reservoir conditions, 60 °C and 3150 psia

10 **Figure 5:** Asphaltene particle size, which are precipitated during pure CO₂ injection at reservoir
11 conditions

12 **Figure 6:** Asphaltene particle size, which are precipitated during DAI/CO₂ injection at reservoir
13 conditions

14 **Figure 7:** The effect of DAI on asphaltene Deposition and decreasing the formation damage: a)
15 pure CO₂ injection and b) CO₂/DAIs injection

16

17

18

19

20

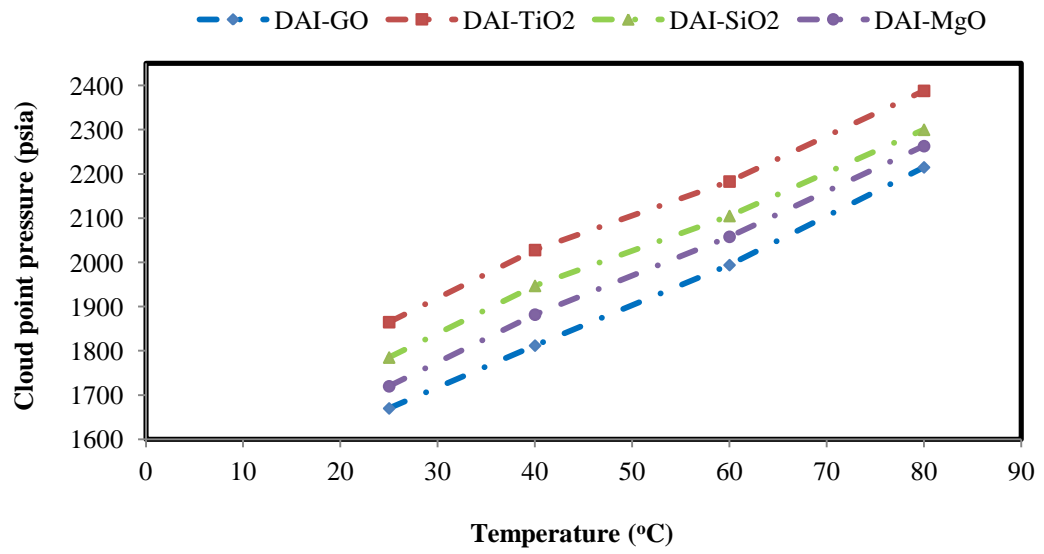
21

22

23

24

1
2
3
4
5
6



7
8
9
10
11
12
13
14
15
16
17

Figure 1

1
2
3
4
5

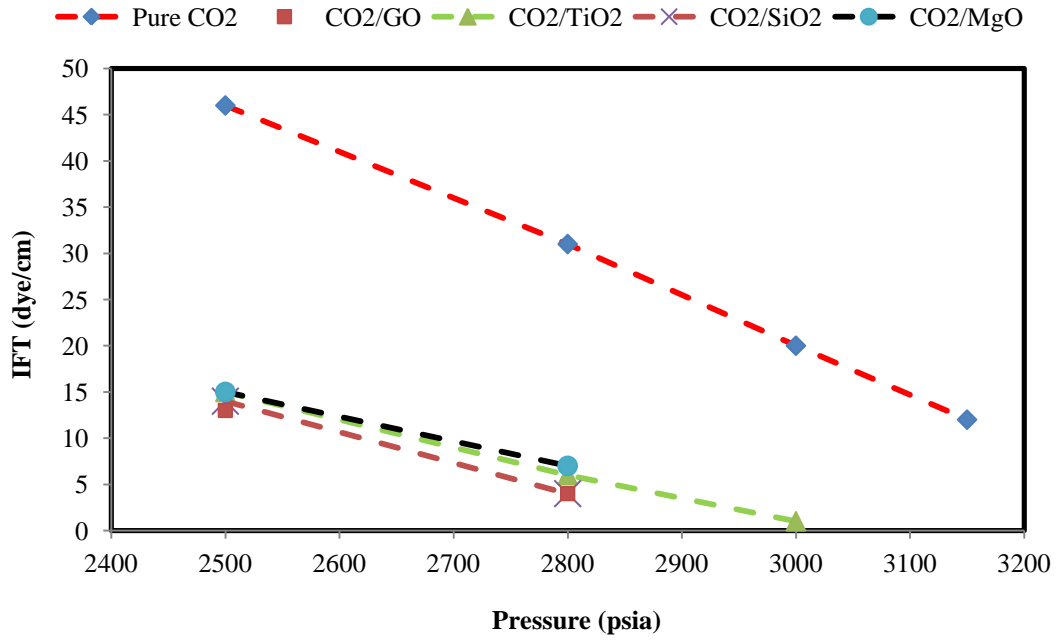


Figure 2

6
7
8
9
10
11
12
13
14
15
16

1
2
3
4
5

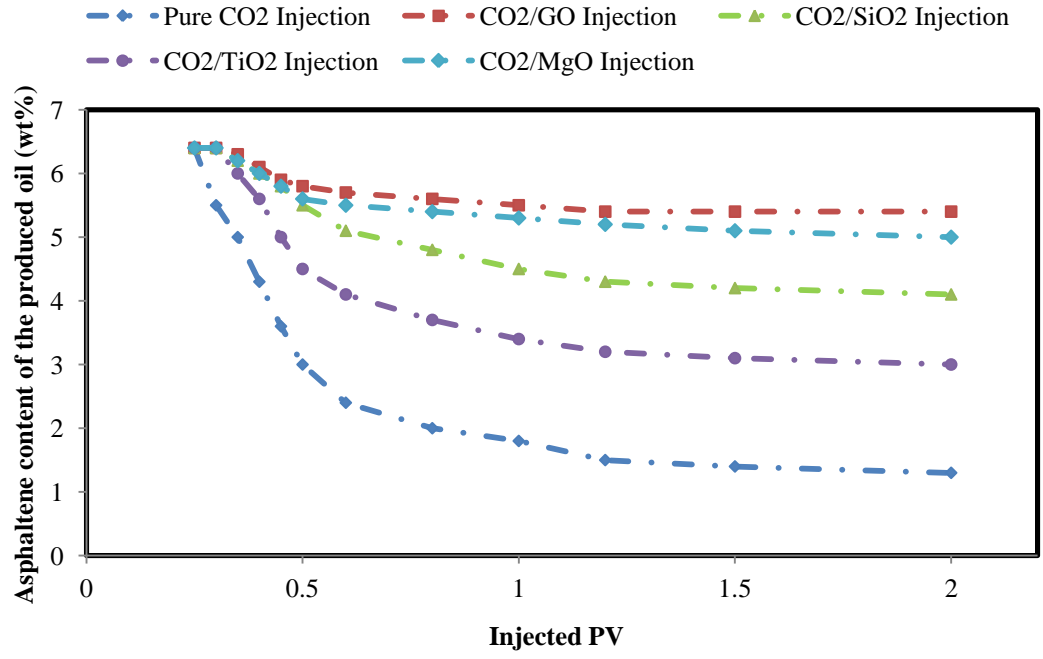
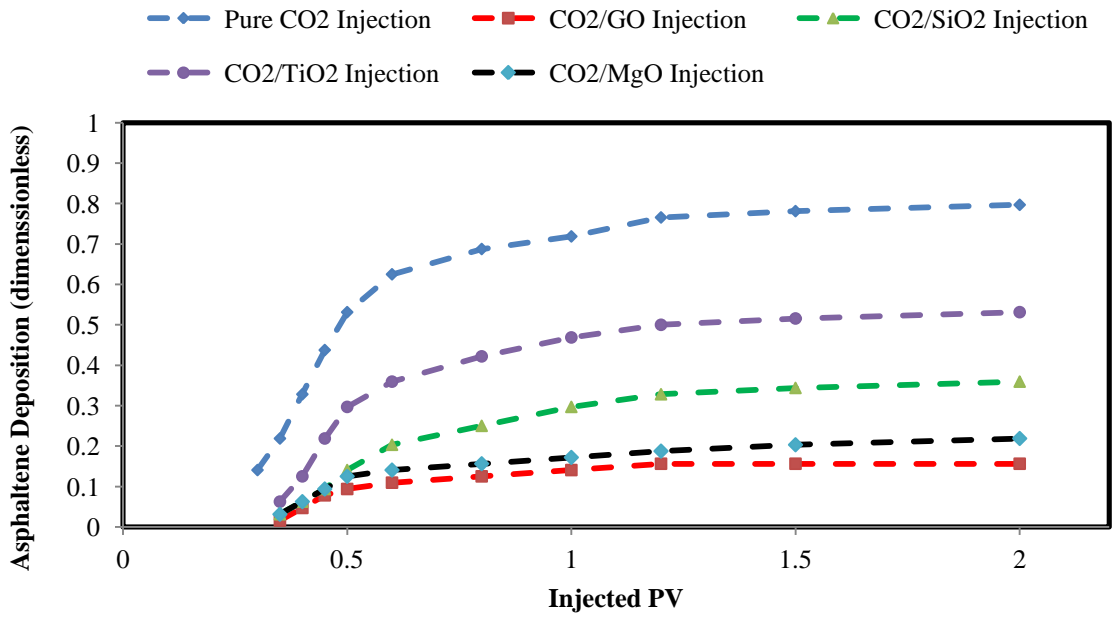


Figure 3

6
7
8
9
10
11
12
13
14
15

1
2
3
4
5



6
7
8
9
10
11
12
13
14

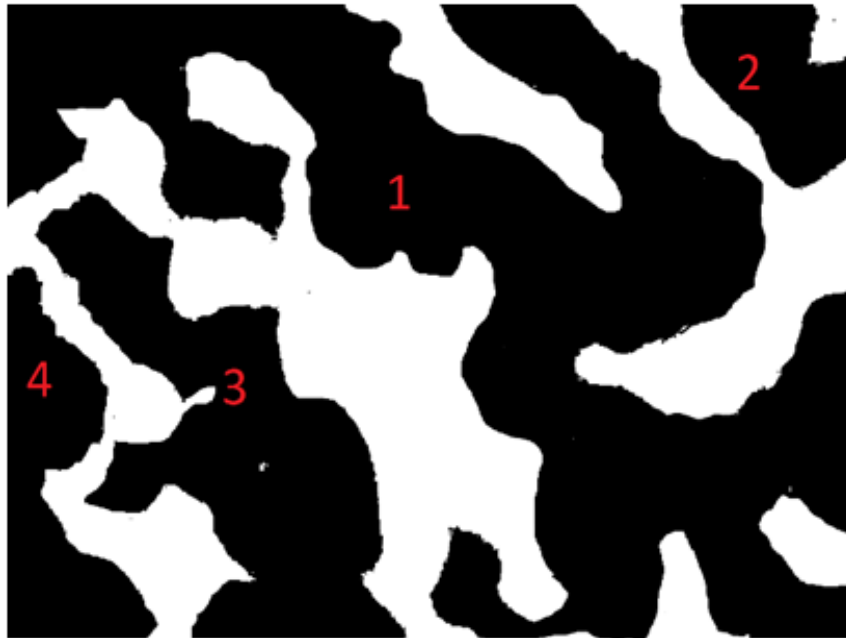
Figure 4

1

2

3

4



Particle number	1	2	3	4
Area (μm^2)	1741670	157860	534393	223885
Total area (μm^2)	2657808			

5

6

7

8

9

10

11

Figure 5

1
2
3
4
5
6
7



Particle number	1	2	3	4	5	6	7	8	9	10
Area (μm^2)	29798	74005	53573	73264	68014	102846	104938	75591	125733	48830
Total area (μm^2)	756592									

8

Figure 6

9

10

11

12

13

14

15

16

17

1
2
3
4
5
6
7
8

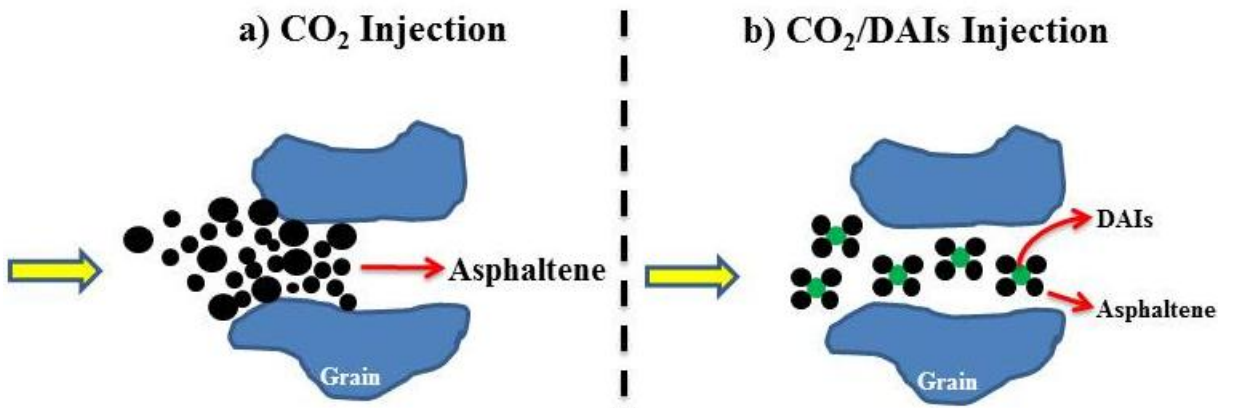


Figure 7

9
10
11
12
13
14

Declaration of interests

The authors declare that they have no known competing financial interests or personal relationships that could have appeared to influence the work reported in this paper.

The authors declare the following financial interests/personal relationships which may be considered as potential competing interests:

Credit author statement

Asghar Gandomkar: Conceptualization, Methodology, Validation, Investigation, Resources, Writing - Original Draft, Writing - Review & Editing, Visualization, Supervision, Project administration. **Hamid Reza Nasriani:** Methodology, Investigation, Writing - Original Draft, Writing - Review & Editing.